AD-A051 340 NAVAL SURFACE WEAPONS CENTER WHITE OAK LAB SILVER SP--ETC F/G 20/4
TEMPERATURE-STEP EFFECTS ON DIRECT MEASUREMENT OF SKIN-FRICTION--ETC(U)
JUL 77 R L VOISINET

UNCLASSIFIED NSWC/WOL/TR-77-7 NL

| OF |
AD
A051 340

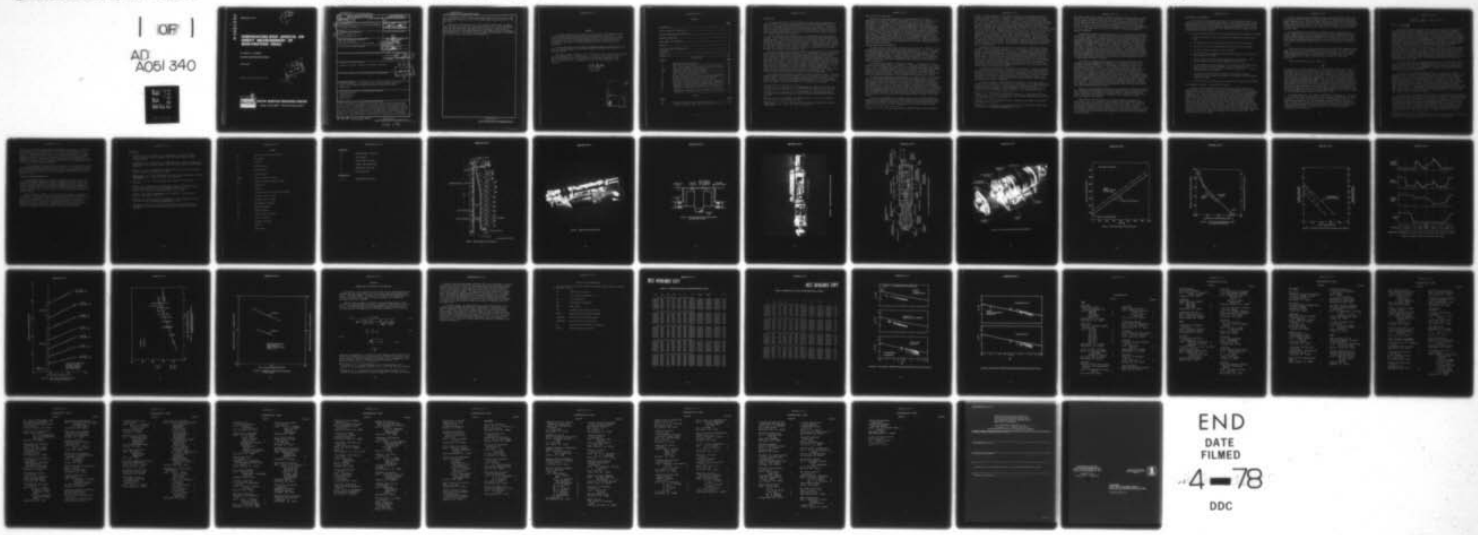

END
DATE
FILMED
4-78
DDC

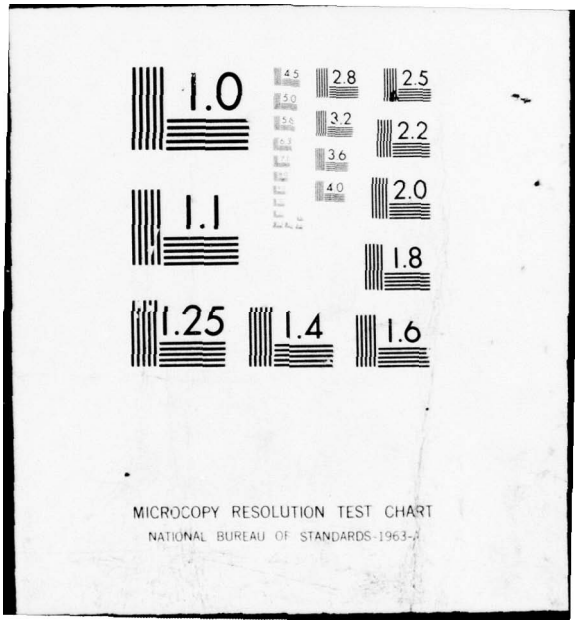
1.0
1.1
1.25
1.4
1.6
1.8
2.0
2.2
2.5
2.8
3.2
3.6
4.0
4.5
5.0
5.6
MICROCOPY RESOLUTION TEST CHART
NATIONAL BUREAU OF STANDARDS-1963-A

AD A051340

NSWC/WOL TR 77-7

12

TEMPERATURE-STEP EFFECTS ON DIRECT MEASUREMENT OF SKIN-FRICTION DRAG

BY ROBERT L. P. VOISINET

ADVANCED WEAPONS DEPARTMENT

7 JULY 1977

DDC
MAR 17 1978
F

Approved for Public Release; Distribution Unlimited

NAVAL SURFACE WEAPONS CENTER

Dahlgren, Virginia 22448 • Silver Spring, Maryland 20910

UNCLASSIFIED

SECURITY CLASSIFICATION OF THIS PAGE *(When Data Entered)*

REPORT DOCUMENTATION PAGE

READ INSTRUCTIONS BEFORE COMPLETING FORM

1. REPORT NUMBER: NSWC/WOL/TR-77-7
2. GOVT ACCESSION NO.
3. RECIPIENT'S CATALOG NUMBER

4. TITLE (and Subtitle): TEMPERATURE-STEP EFFECTS ON DIRECT MEASUREMENT OF SKIN-FRICTION DRAG.

5. TYPE OF REPORT & PERIOD COVERED: Final rept. 1 Jul 76-31 Sep 77

6. PERFORMING ORG. REPORT NUMBER

7. AUTHOR(s): Robert L. P. Voisinet

8. CONTRACT OR GRANT NUMBER(s)

9. PERFORMING ORGANIZATION NAME AND ADDRESS
Naval Surface Weapons Center
White Oak Laboratory
White Oak, Silver Spring, Maryland 20910

10. PROGRAM ELEMENT, PROJECT, TASK AREA & WORK UNIT NUMBERS
61153N; WR02302
WR02302003; WA8201;

11. CONTROLLING OFFICE NAME AND ADDRESS

12. REPORT DATE: 7 Jul 1977

13. NUMBER OF PAGES: 36

14. MONITORING AGENCY NAME & ADDRESS *(if different from Controlling Office)*

15. SECURITY CLASS. *(of this report)*: Unclassified

15a. DECLASSIFICATION/DOWNGRADING SCHEDULE

16. DISTRIBUTION STATEMENT *(of this Report)*

Approved for public release; distribution unlimited

17. DISTRIBUTION STATEMENT *(of the abstract entered in Block 20, if different from Report)*

DDC
RECEIVED
MAR 17 1978
F

18. SUPPLEMENTARY NOTES
Excerpts presented at the FRG/USAF Data Exchange Agreement Meeting on "Viscous and Interacting Flow Field Effects", 28-29 April 1976, WPAFB, Ohio

19. KEY WORDS *(Continue on reverse side if necessary and identify by block number)*
Skin-friction drag
Temperature step
Boundary layer
Shear stress

20. ABSTRACT *(Continue on reverse side if necessary and identify by block number)*

Wall-temperature discontinuities can occur in skin-friction balance tests whenever a balance drag element is thermally insulated from the surrounding test surface. An experimental study was conducted to investigate the effects of such a temperature step on the local friction drag. A temperature step was produced by varying the temperature of the NSWC skin-friction-balance drag element above the temperature of the surrounding nozzle wall. Drag-element temperatures ranged from 100°K to 240°K with the surrounding wall maintained →

DD FORM 1 JAN 73 1473 EDITION OF 1 NOV 65 IS OBSOLETE
S/N 0102-014-6601

UNCLASSIFIED
SECURITY CLASSIFICATION OF THIS PAGE *(When Data Entered)*

391 596

at a temperature of 89°K. Nominal Mach numbers were 2.9 and 4.9 over a unit Reynolds number range of 2.6 to 20 million per meter (0.8 x 10^6 to 6.0 x 10^6 per foot).

The results show that the value of the measured shear stress is higher than the cold wall value for a drag element which is at a higher temperature than the surrounding wall temperature and the change in shear stress is proportional to the difference between the drag element and the surrounding wall temperatures. The data has been correlated and corrections to previously published skin-friction results are presented.

SUMMARY

This report documents the results of an experimental investigation of local surface-temperature-discontinuity effects on measured wall shear stress. The results are correlated and previously published skin-friction data are adjusted to compensate for this drag-element temperature effect. Design modifications and updated capabilities of the NSWC designed skin-friction device are also presented.

The work described in this report was performed under the sponsorship of the Naval Air Systems Command, TASK A320-320C/004A/7R023-02-003 with Mr. Volz as project monitor.

The author wishes to thank Dr. W. J. Yanta and Dr. R. E. Lee for their support and consultation, Mr. J. R. Bruno and Mr. T. Young for their design efforts in improving the NSWC skin-friction balance to its present configuration, and Mr. F. W. Brown and Mr. F. C. Kemerer for their efficient operation of the facility.

C. A. Fisher

C. A. FISHER
By direction

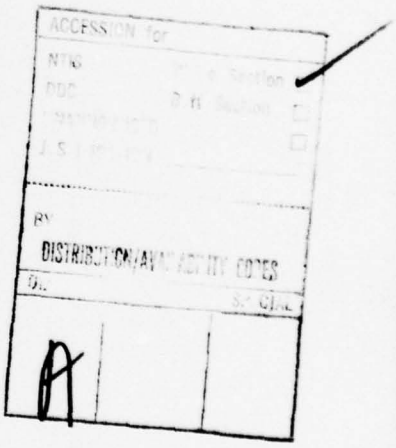

CONTENTS

ILLUSTRATIONS

TABLES

INTRODUCTION

It is well known that a local discontinuity in the surface temperature of a body in motion will markedly influence the heat transfer from the fluid to the body over the region where the discontinuity exists. This effect is especially evident in plug-type calorimeters in high-speed wind-tunnel testing. A similar local "hot spot" condition can occur in skin-friction balance testing when a skin-friction balance drag element is thermally insulated from the cooled or heated main surface surrounding the element.

In the simulation of high-speed flight in a ground test facility where heat transfer is of consideration, the ratio of the wall-to-stagnation temperature is usually matched. The ratio can be attained in a wind tunnel either by raising the stagnation temperature of the facility or cooling the model surface. It has been the practice at NSWC to employ the latter approach in previous experimental studies of the turbulent boundary layer with heat transfer. Temperature ratios as low as 0.2 have been attained by the cryogenic cooling of the nozzle wall in the NSWC Boundary Layer Channel (see References 1 and 2).

From the inception of the cold-wall tests it was realized that a skin-friction balance would be needed which could operate in a cryogenically cooled environment. Such a balance was designed and built (see Reference 3) with a provision for cooling the drag element to the surrounding test-plate temperature just prior to data acquisition. This was to be done by clamping a cryogenically cooled manifold around the drag element. Unfortunately, this provision was not operational during the original tests and the drag element reached a temperature during each test run which was some 150°K hotter than the surrounding test-plate temperature. Since the effects of such a temperature step were unknown, the drag-element cooling capability had to be made operational in order to validate the previous test data. Through numerous balance design modifications and improvements, this cooling capability was made operational and validation tests were performed.

The present report describes the results of those validation tests. The drag-element temperature data are correlated and this correlation is applied to earlier published data. The data of Westkaemper (Reference 4) agree with the present results; however, the conclusion reached by that author; i.e., negligible temperature step effects, are not consistent with the findings of this study.

---

[1] Voisinet, R. L. P., and Lee, R. E., "Measurements of a Mach 4.9 Zero-Pressure Gradient Turbulent Boundary Layer with Heat Transfer," NOLTR 72-232, Sep 1972.

[2] Voisinet, R. L. P., and Lee, R. E., "Measurements of a Supersonic Favorable-Pressure-Gradient Turbulent Boundary Layer with Heat Transfer," NOLTR 73-224, Dec 1973.

[3] Bruno, J. R., et. al., "Balance for Measuring Skin Friction in the Presence of Heat Transfer," NOLTR 69-56, Jun 1969.

[4] Westkaemper, J. C., "Step Temperature Effects on Direct Measurements of Drag," AIAA Journal, Vol. 1, No. 7, Jul 1963, pp. 1708-1710.

FACILITY AND TEST CONDITIONS

Wind-tunnel tests were conducted in the NSWC Boundary Layer Channel (Reference 5) at nominal freestream Mach numbers of 2.9 and 4.9. Skin-friction measurements were made on the flat nozzle-wall test plate of the facility (see Figure 1). The copper test plate was cryogenically cooled with liquid nitrogen to a temperature of 89°K. The supply temperatures were nominally 422°K and 403°K at the Mach 4.9 and 2.9 conditions respectively. The test conditions for the Mach 4.9 case were essentially the same as those reported in Reference 1 since the present tests were conducted for the purpose of validating the previous test data. The Mach 2.9 test conditions were similar except for a change in nozzle contour. The Reynolds number was varied by changing the supply pressure from 1 to 10 atmospheres at Mach 4.9 and 1 to 2 atmospheres at Mach 2.9. Data were obtained at several axial stations along the test plate. Typical wind-tunnel test runs lasted on the order of 90 minutes with half of that time being used for tunnel cool-down procedures.

BALANCE DESCRIPTION AND OPERATION

The skin-friction balance used in these tests is pictured in Figure 2. It is a redesigned version of the balance described in Reference 3. It is of the self-nulling type whereby a circular floating drag element is continually re-centered by a servo-feedback system. The unique feature of the balance design is the "clam-shell" mechanism used to cool the floating drag element to the temperature of the surrounding test plate. Although the basic design of the new balance is similar to the old, significant modifications have been made in the process of design optimization.

The balance drag element is sketched in Figure 3. It consists of a flat surface circular element which is 2.00533 cm. in diameter (surface area = 3.15836 $cm.^2$). The lip thickness is 0.00762 cm. and the clearance gap around the element is 0.0127 cm. The element edge is beveled at a 45° angle to minimize edge-pressure effects and the element surface is aligned flush with the surrounding flange surface to within $\pm$ 0.001 cm. Since the balance mechanism is of the self-nulling type, the clearance gap around the drag element does not change with loading.

The balance servo-feedback system operates in a manner similar to the previous design. The surface shear stress acting on the drag element causes the balance arm to rotate about a frictionless pivot (refer to the schematic in Figure 4). The movement of the arm is sensed by a translational Linear Variable Differential Transformer (LVDT). The LVDT null-offset signal is monitored by servo-feedback electronics and a DC motor is activated to produce a restoring force to the balance arm via a lead-screw, spring guide, and spring. The force exerted by the restoring spring opposes the shear force and restores the balance arm and drag element to a null or centered position. The magnitude of the restoring force is proportional to the shear force and is monitored by a potentiometer which is geared to the lead-screw.

Since the servo-feedback is a dynamic system; spring, mass and damping components must be adjusted to obtain a stable response to the applied shear loading. The mass of the system is concentrated in the balance arm and counterweight and remains constant except for minor changes which are initially made for static

---

[5] Lee, R. E., et. al., "The NOL Boundary Layer Channel," NOLTR 66-185, Nov 1966.

balance. Spring components in the system are found in the restoring spring and in the frictionless pivots, the flexures. These springs are matched to the drag loading expected in the test. Damping is introduced in the system using a dashpot. This is a change from the original design of damping discs which were developed by Durgin (Reference 6). The dashpot is composed of a small piston housed in a nonferrous cylindrical casing with a clearance gap between the two. The piston is made from a magnet and a magnetic damping fluid (References 7 and 8) is introduced into the clearance gap. The damping fluid (Dyester base, 10K centipoise viscosity) stays in the gap because of its magnetic attraction to the piston. The size of the piston and gap and the viscosity of the damping fluid determine the amount of viscous damping which is introduced in the system. Electronic damping (filtering) is also used to regulate the overall balance sensitivity and response. The final adjustments to the system are generally made to produce a critically damped response to an applied shear-stress loading. An underdamped system can cause undue oscillations of the balance arm about the null position and an overdamped system can respond too slowly to changes in the loading. The technique of system adjustment is generally one of trial and error.

Preliminary tests showed the balance to be sensitive to temperature changes around the critical balance components, i.e., the flexures, LDVT, springs and aft housing. Since the balance had to be used in a cyrogenically-cooled environment, special precautions were taken to insulate these sensitive components from the extreme cold. The mounting flange and drag-element cooling mechanism which are in direct contact with the cryogenic cooling were thermally insulated from the aft portion of the balance housing to minimize conduction effects. As an added temperature buffer, heater tape was applied to the mid-balance housing to compensate for the extreme cold at the mounting flange. As a result, the aft balance housing temperature remained relatively constant through each test run and thermal effects on the balance calibration were minimal.

The dimensional stability of the balance which relates to component expansion and contraction with temperature was minimized by using Invar and other materials having low coefficients of thermal expansion. Components such as the balance arm and balance housing had to be constructed of these materials otherwise the thermal expansion of the components would have changed the drag-element alignment with the surrounding surface. Maximum variation in surface alignment under cryogenic conditions was less than $\pm$ 0.0025 cm.

In a manner similar to that described in Reference 3, the present balance design has the capability of pre-cooling the drag element to the temperature of the surrounding wall by placing a coolant manifold, a "clam-shell" device, in direct contact with the drag element. The clamping action of the "clam-shell" is accomplished via a pneumatic cylinder, worm gear, and linkages (see Figure 5).

---

[6]Durgin, F. H., "The Design and Preliminary Testing of a Direct Measuring Skin Friction Meter for Use in the Presence of Heat Transfer," Massachusetts Institute of Technology Report 93, Jun 1964

[7]Ezekiel, F. D., "Uses of Magnetic Fluids in Bearings, Lubrication and Damping," ASME Paper 75-DE-5, 1975

[8]Moskowitz, R., "Designing with Ferro-Magnetic Fluids," ASME Paper 74-DE-5, 1974 and reprinted in Mechanical Engineering, Feb 1975

The coolant flows from an external reservoir through an internal network of manifolds, flexible metallic bellows, and the "clam-shells." The mounting flange of the balance is cooled by conduction from the surrounding test plate. When liquid nitrogen was used as the coolant, the drag element could be cooled to within 15°K of the surrounding test-plate temperature. Since the drag element is made of copper and has a relatively large thermal capacity, its temperature did not rise at any significant rate after the release of the cooling manifold.

BALANCE CALIBRATION

The balance was easily calibrated because of its orientation when mounted in the vertical wind tunnel. Standard weights were directly attached to the surface of the drag element and the resultant force acted in a direction tangent to the drag-element surface. The balance response to the applied force was monitored by measuring the voltage output across the balance potentiometer. The balance was adjusted to accommodate loading as high as 3000 mg for the Mach 2.9 tests and 1500 mg for the Mach 4.9. Calibrations (as shown in Figure 6) were represented by straight lines with the "zero," no-load intercept, and "slope," voltage per milligram of loading, being the calibration constants. The calibration "slope" which was a function of the restoring spring constant and potentiometer voltage setting, changed very little between test runs, and proved to be very stable for a particular balance configuration. The calibration "zero" constant which relates to the no-load output of the balance varied with aft housing temperature and to a lesser degree with static pressure.

The effects of temperature and pressure on the balance calibration were evaluated in an environmental test chamber prior to wind-tunnel testing. By changing the ambient temperature of the balance, a calibration "zero" shift was measured as shown in Figure 7. This calibration shift was primarily a result of thermal effects on the sensitive balance components housed in the aft portion of the balance. As was noted earlier, the aft balance housing was maintained at a relatively constant temperature during a wind-tunnel test run to minimize the temperature change and the resulting errors. The balance housing temperature was monitored during each wind-tunnel test and if a temperature change occurred, appropriate corrections were made to the calibration "zero" constant. For the longest of wind-tunnel test runs the aft housing temperature changed by less than 3°K. The no-load "zero" reading was monitored just prior to and just after each air flow cycle allowing for a relatively short time and small temperature change between calibration checks.

Changes in the drag-element temperature did not affect the balance calibration. This was determined by obtaining no-load and loaded calibration checks before and after activation of the "clam-shell" cooling manifold. Both the calibration "zero" and "slope" were found to be unaffected by the temperature changes of the mounting flange and drag element.

The effects of static pressure on the newly designed balance were not significant. This is in contrast to the problems noted in Reference 3 where a sizable calibration "zero" shift resulted with pressure change. The reason for the previous problem related to the LVDT and the way in which it has been electronically excited. Present calibration results are shown in Figure 8. Since a calibration "zero" reading was taken before and after each wind-tunnel test run at a low pressure near the flow static pressure, a correction to the calibration was not necessary.

WIND-TUNNEL TEST PROCEDURE

The skin-friction balance was made to fit the instrumentation ports in the copper test plate of the Boundary Layer Channel. The aft portion of the balance projected back into the plenum chamber of the facility where associated wiring, liquid nitrogen supply lines, and pressure leads were attached. The aft portion of the balance was sealed, eliminating air leakage through the balance from the plenum of the test-plate surface.

For each wind-tunnel test run the following procedures were generally followed:

1. Prior to each run, a check of drag-element alignment and centering was made.

2. The balance was load calibrated while installed in the test plate.

3. The facility doors were closed and the test section was evacuated.

4. The test plate was cooled with liquid nitrogen.

5. Once the test-plate temperature was achieved uniformly, the balance "no load" output was recorded.

6. The air flow was started and drag measurements were obtained. Both Reynolds number and drag-element temperature were cycled.

7. At the completion of data acquisition, the tunnel was shut down and the liquid nitrogen cooling was stopped. A no-flow condition was established at a low test section pressure and temperature. A balance "no-load" output was recorded.

8. The test-section pressure was elevated to atmospheric pressure conditions, facility doors were opened, and a check of the drag-element alignment was made.

9. After a period of facility warmup, a post-test calibration was conducted.

This sequence of events is illustrated in Figure 9.

A number of test parameters were monitored during each wind-tunnel run. These included the wind-tunnel supply pressure and temperature, the test-plate temperature and static pressure, the balance internal pressure, the drag-element temperature, the balance aft-housing temperature, and the balance potentiometer voltage reading. These parameters established aerodynamic and heat-transfer conditions, allowed balance calibration checks, and provided the shear-stress data. The "slope" constant in the balance calibration was assumed constant through each run based on preliminary test results and the calibration checks which were taken before and after each test. The "zero" constant was evaluated from the "no-load" balance readings obtained just before and just after the air-flow cycles (at steps 5 and 7 and at times during step 6 in the procedure). Any changes in the "no-load" readings before and after the run were usually traced to aft housing temperature changes and appropriate corrections were made. This correction was usually minimal.

The shear stress variation with drag-element temperature was obtained in one of two ways; either the Reynolds number was cycled for progressively cooler drag-element temperatures or the drag-element temperature was cycled for set Reynolds number conditions (see Figure 9). Procedure steps 6A and 6B). The latter technique produced more consistent data; however, once the drag element had been cooled over one cycle it took a long time for it to warm up for a second cycle at a different Reynolds number.

The drag element of the skin-friction balance was not cooled during the initial stages of a test run and the drag element reached a temperature which was several hundred degrees above the temperature of the surrounding cooled surface. By obtaining wall shear-stress measurements at this temperature and for successively cooler drag-element temperatures using the "clam-shell" cooling mechanism, surface shear-stress data were obtained over a range of drag-element temperatures.

RESULTS

Typical plots of the surface shear stress versus drag-element temperature are shown in Figure 10 for both the Mach 4.9 and 2.9 conditions. An "ideal" cold-wall shear stress is obtained from an extrapolation of such data to where the drag-element temperature is equal to the surrounding wall temperature. The slope of this extrapolation line gives the shear error per degree of temperature difference.

Since the wall shear stress is defined as

$$\tau_w = \mu \frac{du}{dy} \qquad (1)$$

a discontinuity in surface temperature can influence the surface shear stress through the fluid viscosity and/or the velocity gradient at the wall. Figure 10 shows that the effect of a locally "hot" drag element is to increase the local wall shear stress in proportion to the difference between the drag-element temperature and the surrounding wall temperature. It is easy to see from Equation 1 that the higher the drag-element temperature, the higher the surface viscosity, and the higher the measured wall shear. The effects of a temperature step on the local boundary-layer velocity gradient at the wall cannot be analyzed as directly. Many factors can influence the velocity gradient at the wall, including the size and shape of the drag element, the boundary-layer thickness, the boundary-layer velocity and temperature profiles, the Mach number and the Reynolds number. Over the limited scope of these tests the drag-element geometry and size were unchanged and only the Mach number and Reynolds number were varied.

The shear-stress error per degree of temperature difference, i.e., the slope of the linear variation of shear stress with drag-element temperature, is shown in Figure 11 as a function of Reynolds number. The magnitude of the error is observed to decrease slightly with decreasing Reynolds number for the Mach 4.9 data. At Mach 2.9, only two Reynolds number conditions provided data and no trends could be determined other than the general agreement of the Mach 2.9 data with the Mach 4.9 results. A least-square fit of all the data provided a calibration curve of the form

$$\frac{\tau_{DE} - \tau_w}{T_{DE} - T_w} \left(\frac{N}{M^2\ {}^oK}\right) = A \log_{10} (Re/m) + B \qquad (2)$$

where: A = 0.0310988
B = 0.1795555

The data of Westkaemper (Reference 4) is often referenced on the subject of temperature-step effects. Westkaemper concluded that a moderate temperature mismatch (maximum of 34^oK) produced a negligible effect on the drag (less than 2 percent) over the range of test conditions covered in that study (Mach 5, Reynolds number per meter from 16.5 to 25 million). If the present correlation (Equation 2) is evaluated for the conditions of Westkaemper's tests (Mach 5, $Re/m = 20. \times 10^6$), a wall shear stress error of 0.0475 N/m^2 per ^oK is indicated. For a 34^oK maximum temperature step and a nominal wall shear stress of 82.1 N/m^2 (C_f assumed equal to 0.0015), the wall shear stress variation which might be expected from the present correlation would be of the order of 1.96 percent. This low percentage error is within the observed drag variation and stated experimental accuracy noted by Westkaemper. As such, if the present correlation were to hold for those tests, the expected error would be small, it would be very difficult to evaluate and could easily be over-shadowed by the accuracy limitations of the experiment. The temperature-step effects might be considered negligible for those tests; however, the inference that the temperature-step effects are generally negligible must not be made.

It has been shown that the absolute magnitude of wall shear-stress error per degree of temperature mismatch is not a strong function of the wall shear stress (see Figure 11). As such, the percentage error will be small if the absolute magnitude of the wall shear stress is large. However, the opposite will be true for small values of wall shear stress.

The magnitude of the temperature-step effects in these tests is better realized in Figure 12 where the calibration results are presented in terms of the percentage error. Errors as high as 0.45 percent per degree (K) of temperature mismatch are indicated. The percentage errors are higher at the higher Mach number conditions because the wall shear stress is lower for the same Reynolds number (the absolute error showed no dependence on Mach number). For a constant Mach number, the percentage error increases with decreasing Reynolds number. Again the magnitude of the percentage errors tends to reflect the magnitude of the wall shear stress. It is important to note that the percentage errors can become very large as the value of the wall shear stress becomes small; i.e., for high Mach numbers and/or low Reynolds numbers.

As a final note, some comment should be made as to drag-element misalignment and the possibility of errors resulting from such misalignment. Several precautions were taken to minimize this problem as discussed in the text and, for the most part, the steps taken were successful. The drag-element misalignment was less than $\pm$ 0.0025 cm, and based on the data of O'Donnell (Reference [9]) an error in shear stress of less than $\pm$ 4 percent could be expected. Between duplicate test runs and for certain long test runs where the temperature of the drag-element was cycled several times, the level of shear stress was slightly different between temperature cycles. These shifts could not always be explained in terms of

[9] O'Donnell, Francis B., Jr., "A Study of the Effect of Floating Element Misalignment on Skin-Friction-Balance Accuracy," DRL Report 515, CR-10, Mar 1964

calibration shifts and a drag-element misalignment was suggested. It should be noted, however, that the data showed a consistent trend of decreasing shear stress with decreasing temperature for each of the temperature cycles. Also, the shift in shear stress which was due to suspected misalignment of the drag element was always less than the change in shear stress due to drag-element temperature effects. Since the data were analyzed for single temperature cycles, changes in the shear-stress value between cycles were not considered and effects on the analysis were considered minimal.

Since the purpose of these tests was to obtain a calibration which could be used to verify previously published skin-friction data, it is appropriate that the calibration now be applied to that data. Refer to Appendix A for a listing and description of corrections which were applied to the skin-friction data of References 1 and 2.

CONCLUSIONS AND RECOMMENDATIONS

An experimental study was conducted to determine the NSWC skin-friction balance drag-element temperature effects on measured wall shear stress. The results of the study indicate a friction-drag variation which is proportional to the difference between the drag-element temperature and the temperature of the surrounding wall. The percentage change can become very large when the value of the wall shear stress is low, i.e., for high Mach numbers and/or low Reynolds numbers.

Additional work is needed to gain a better understanding of temperature-step effects. The present study has shown that an effect exists and this effect can be significant. Other experimentalists must now consider this fact and evaluate the effects for their balance configuration and flow-field conditions. Of equal importance to experimental results is the need for analytic modeling of the effect. Hopefully from an analytic approach, the important parameters which influence the effect may be determined.

REFERENCES

1. Voisinet, R. L. P., and Lee, R. E., "Measurements of a Mach 4.9 Zero-Pressure-Gradient Turbulent Boundary Layer with Heat Transfer," NOLTR 72-232, Sep 1972

2. Voisinet, R. L. P., and Lee, R. E., "Measurements of a Supersonic Favorable-Pressure-Gradient Turbulent Boundary Layer with Heat Transfer," NOLTR 73-224, Dec 1973

3. Bruno, J. R., et. al., "Balance for Measuring Skin Friction in the Presence of Heat Transfer," NOLTR 69-56, Jun 1969

4. Westkaemper, J. C., "Step Temperature Effects on Direct Measurements of Drag," AIAA Journal, Vol. 1, No. 7, Jul 1963, pp. 1708-1710

5. Lee, R. E., et. al., "The NOL Boundary Layer Channel," NOLTR 66-185, Nov 1966

6. Durgin, F. H., "The Design and Preliminary Testing of a Direct Measuring Skin Friction Meter for Use in the Presence of Heat Transfer," Massachusetts Institute of Technology Report 93, Jun 1964

7. Ezekiel, F. D., "Uses of Magnetic Fluids in Bearings, Lubrication and Damping," ASME Paper 75-DE-5, 1975

8. Moskowitz, R., "Designing with Ferro-Magnetic Fluids," ASME Paper 74-DE-5, 1974 and reprinted in Mechanical Engineering, Feb 1975

9. O'Donnell, Francis B., Jr., "A Study of the Effect of Floating Element Misalignment on Skin-Friction-Balance Accuracy," DRL Report 515, CR-10, Mar 1964

SYMBOLS

C_f	local skin-friction coefficient
M	Mach number
P	pressure
P_s	static pressure
P_{t_2}	Pitot pressure
r	recovery factor
Re/m	Reynolds number per meter
Re_θ	momentum thickness Reynolds number
T	temperature
u	velocity
x	distance along plate from nozzle throat
y	distance normal to plate
δ	boundary-layer thickness
δ^*	displacement thickness
θ	momentum thickness
θ_E	energy thickness
θ_H	total enthalpy thickness
μ	dynamic viscosity
ν	kinematic viscosity
ρ	density
τ	shear stress

Subscripts

aw	adiabatic-wall conditions
DE	drag element
e	free-stream conditions
o	tunnel supply conditions
t	stagnation conditions
w	wall conditions

Superscripts

$\overline{\quad}$	transformed quantities

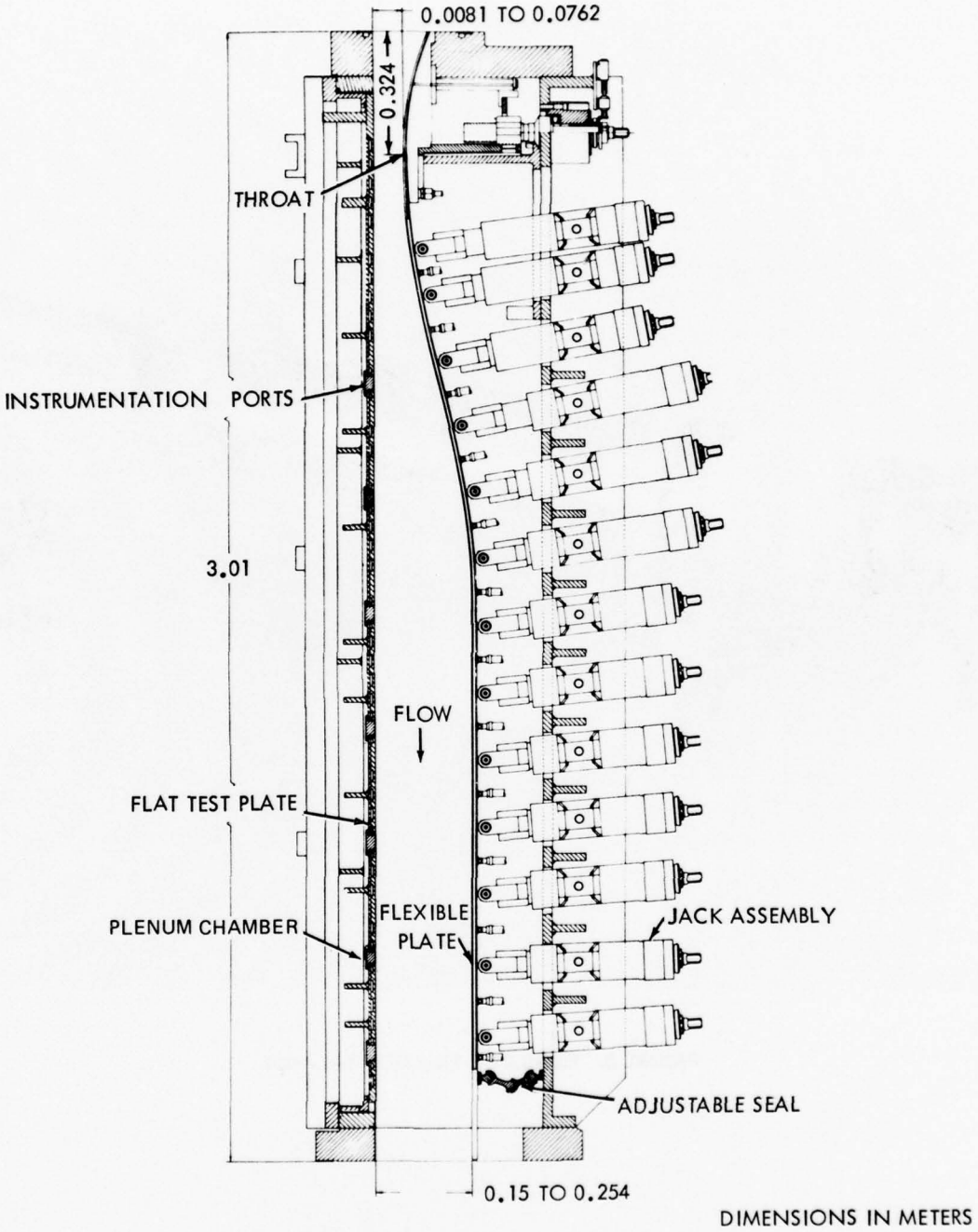

FIGURE 1 NSWC BOUNDARY LAYER CHANNEL

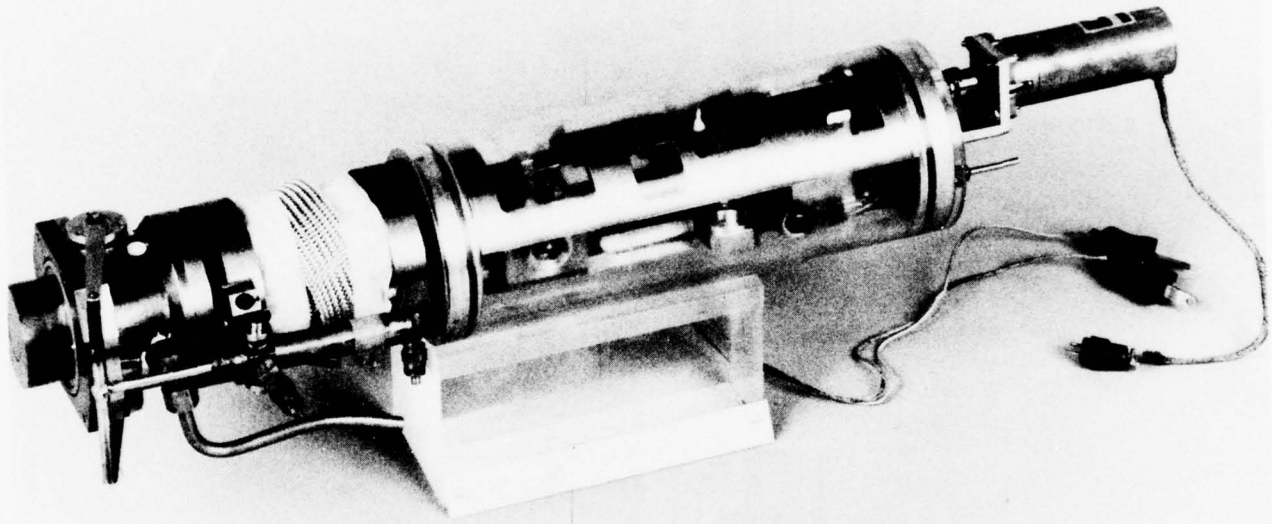

FIGURE 2 NSWC SKIN-FRICTION BALANCE

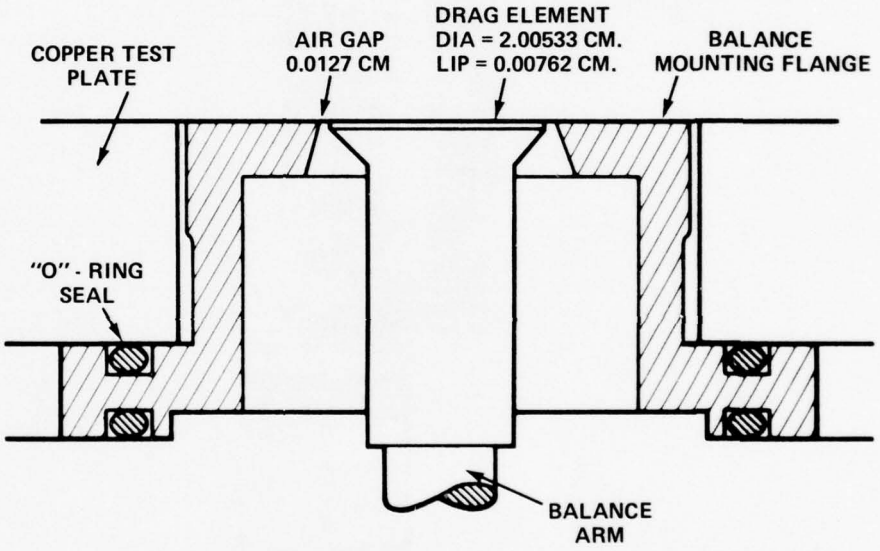

FIGURE 3 SKIN FRICTION BALANCE DRAG ELEMENT AND MOUNTING FLANGE

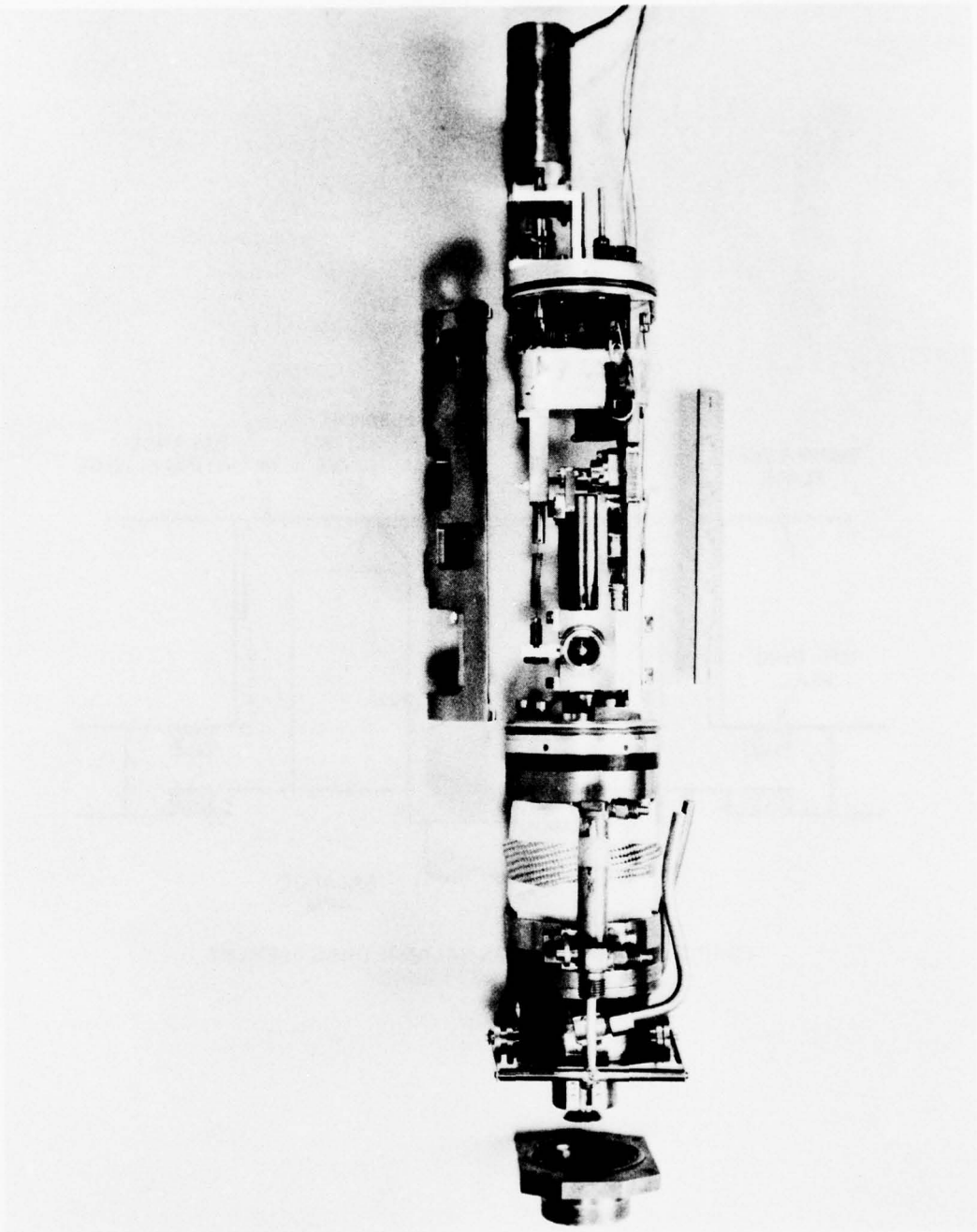

FIGURE 4(a) PHOTOGRAPH, NSWC SKIN-FRICTION BALANCE

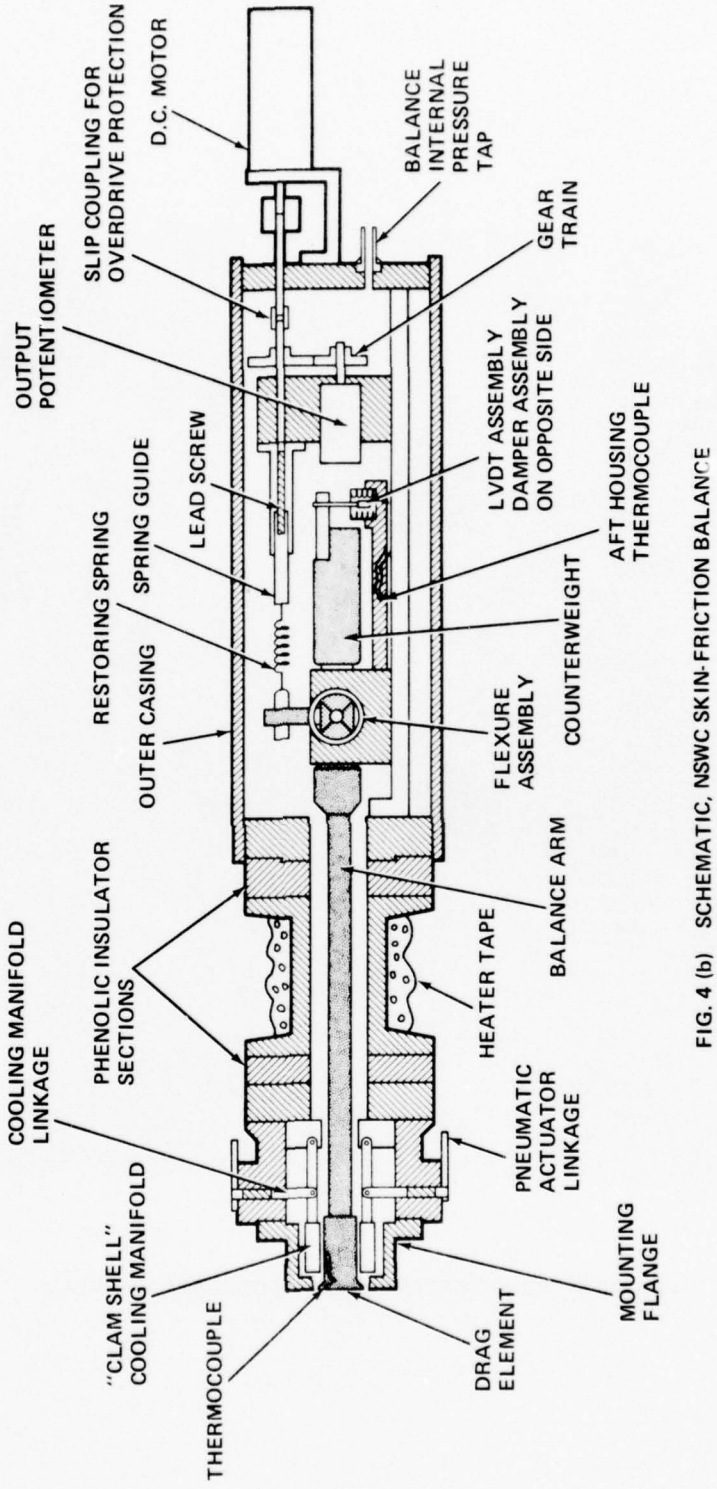

FIG. 4 (b) SCHEMATIC, NSWC SKIN-FRICTION BALANCE

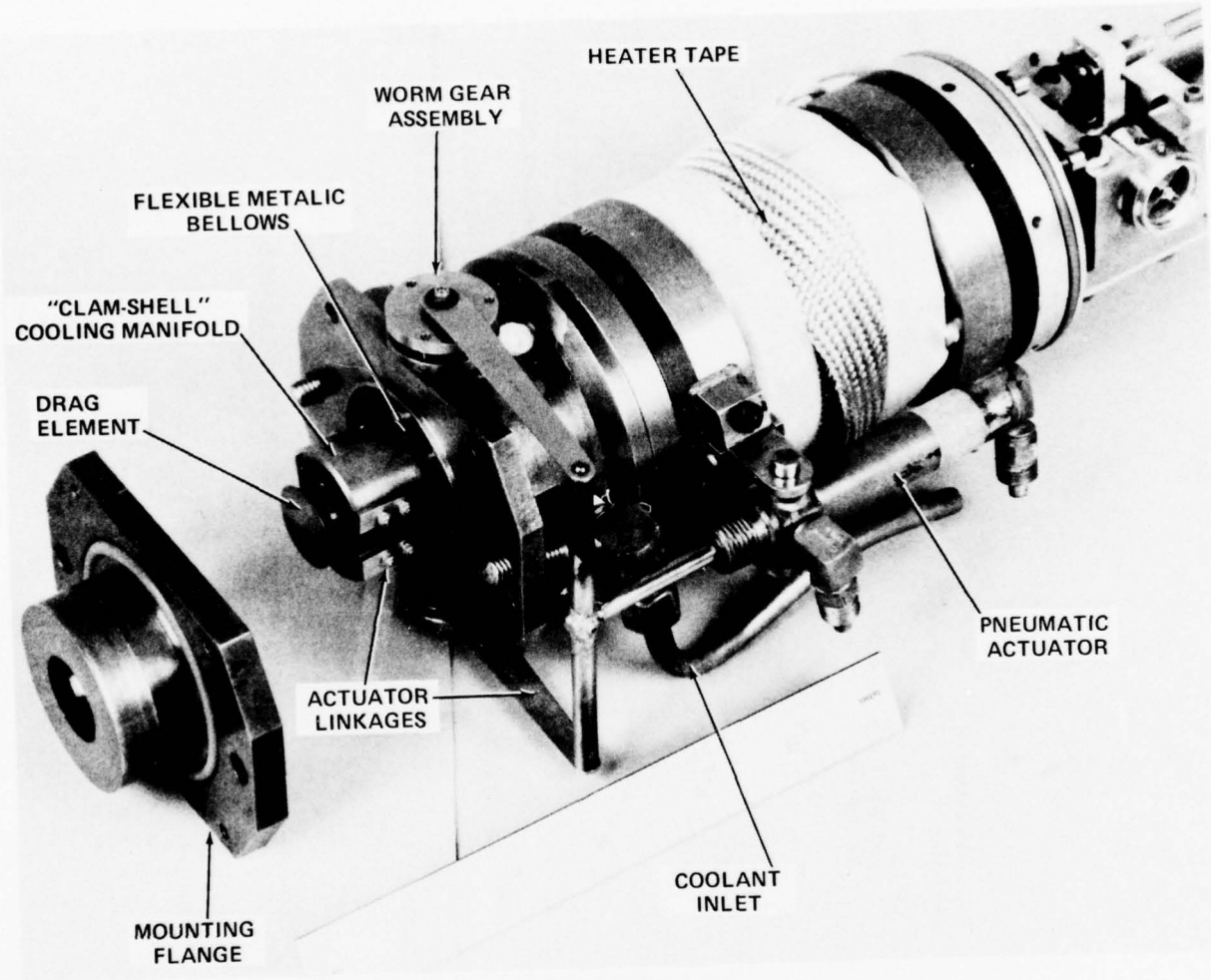

FIGURE 5 SKIN FRICTION BALANCE COOLING ASSEMBLY

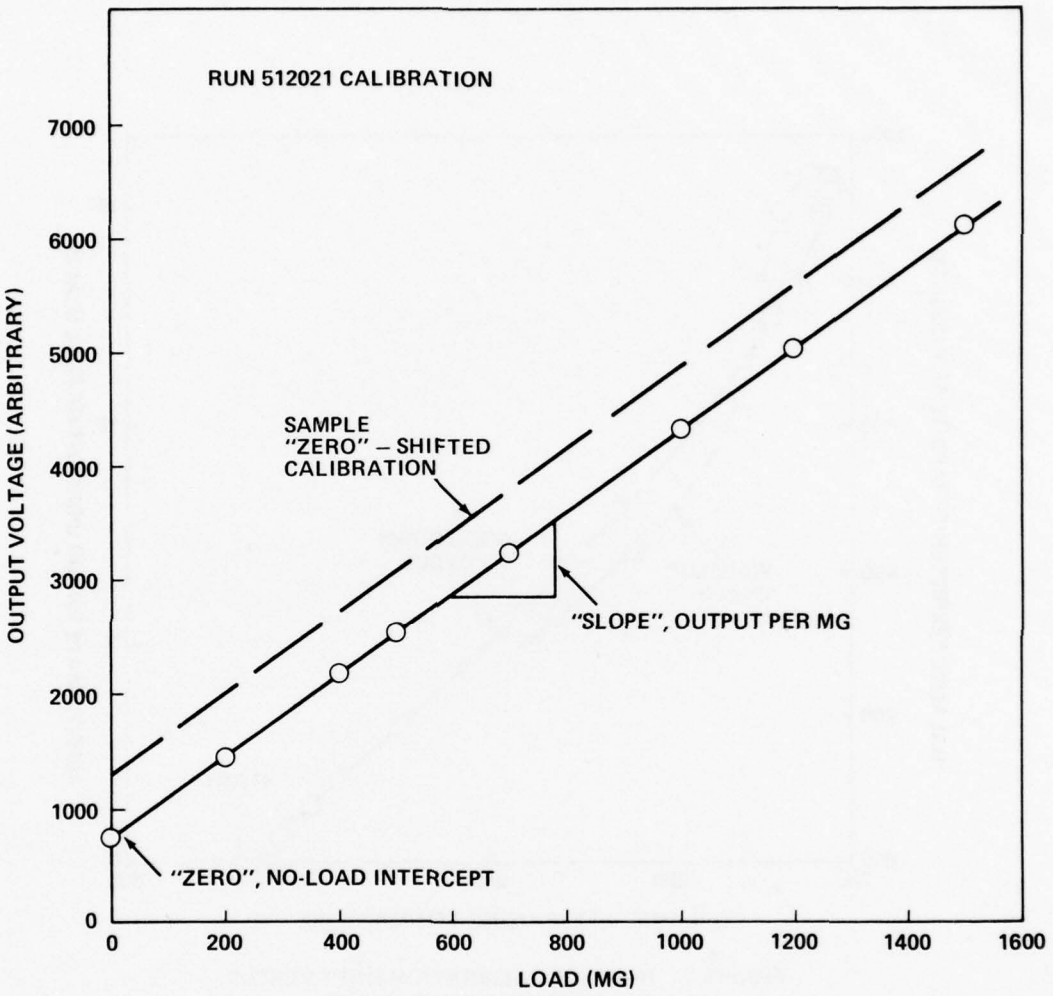

FIGURE 6 SAMPLE BALANCE LOAD CALIBRATION

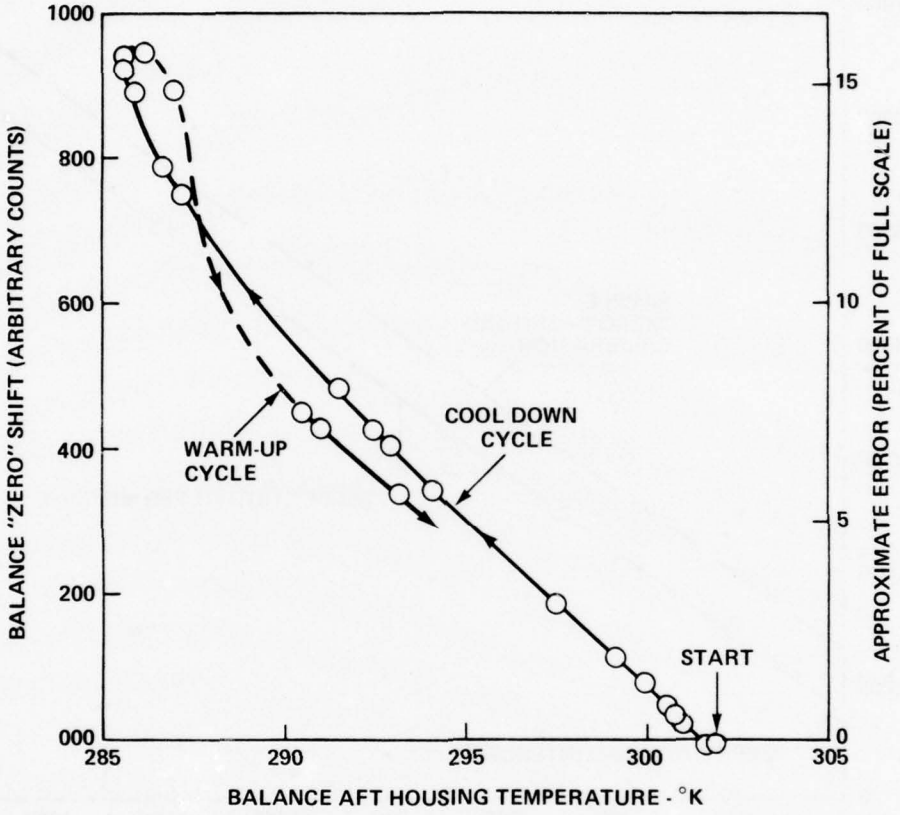

FIGURE 7 BALANCE CALIBRATION SHIFT VERSUS AFT HOUSING TEMPERATURE

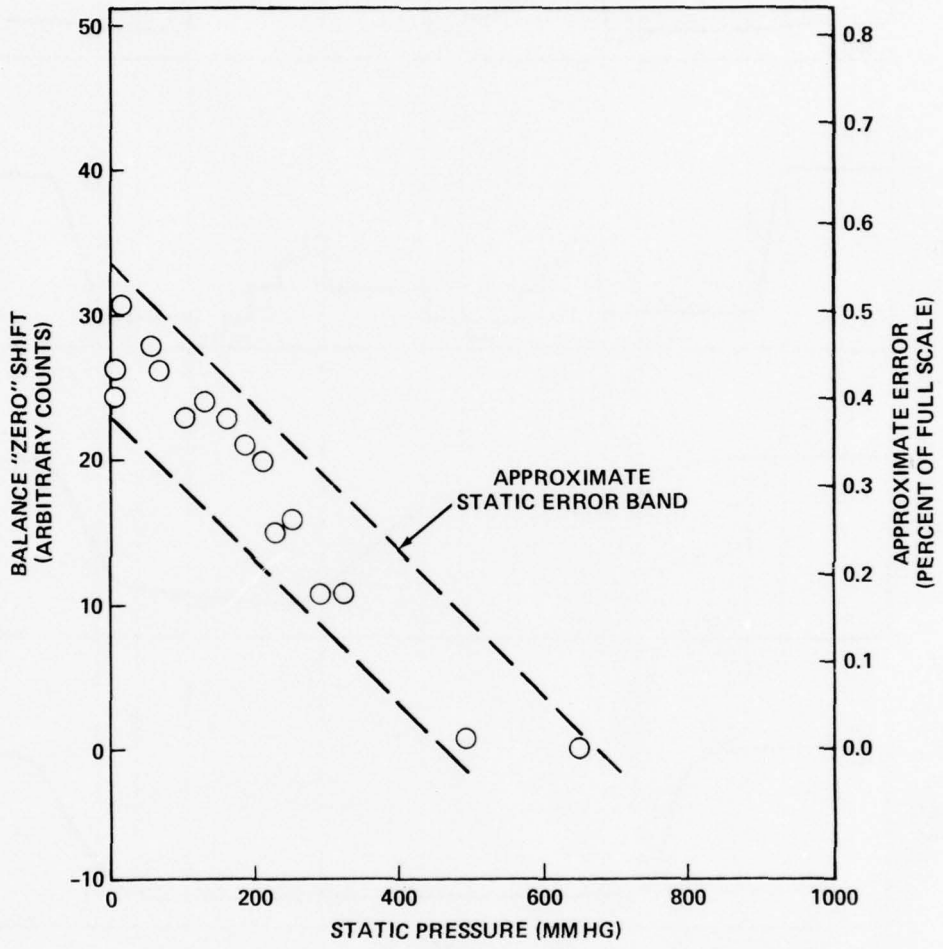

FIGURE 8 BALANCE CALIBRATION SHIFT VERSUS STATIC PRESSURE

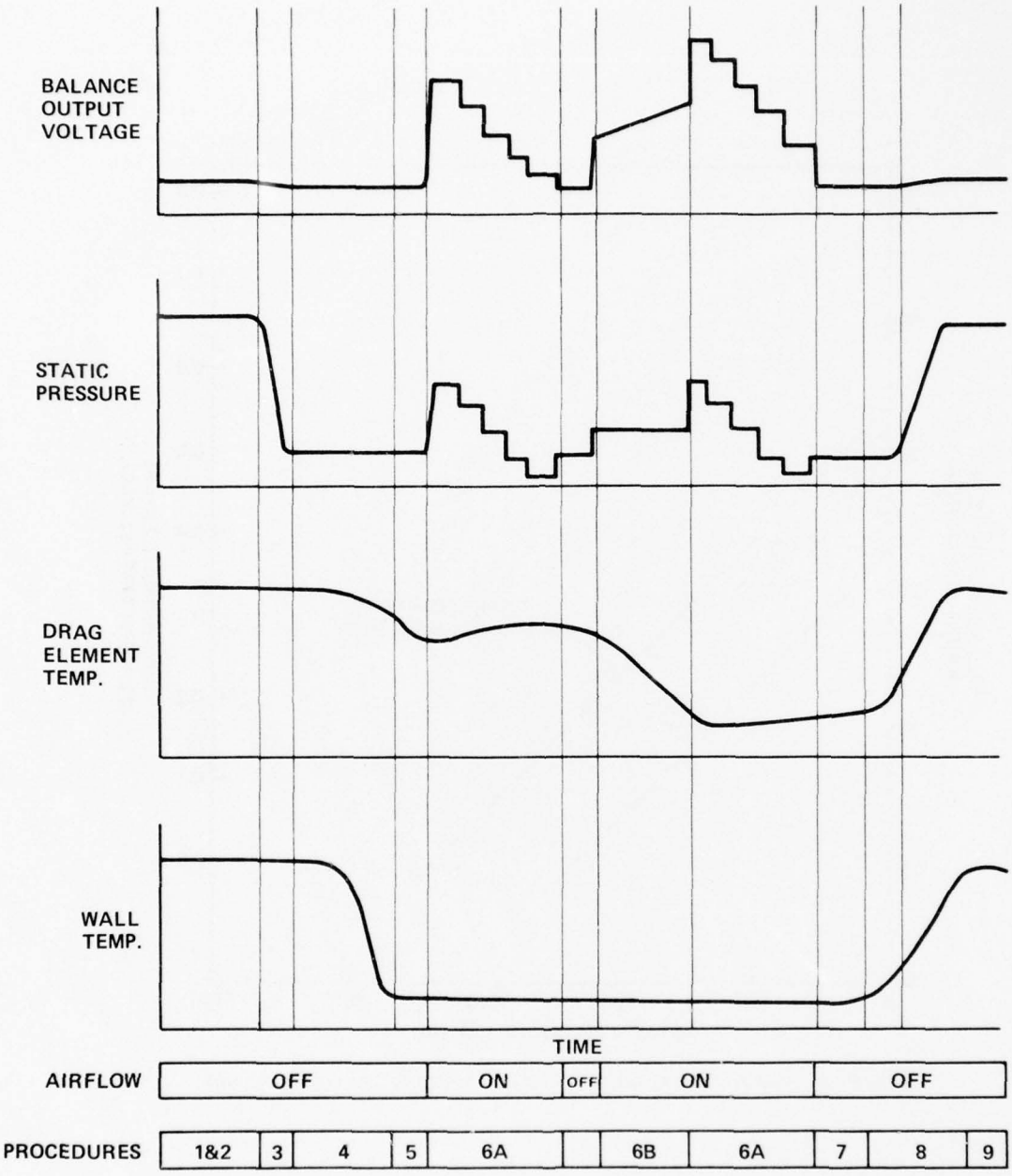

FIGURE 9 SEQUENCE OF EVENTS DURING TEST (NOT TO SCALE)

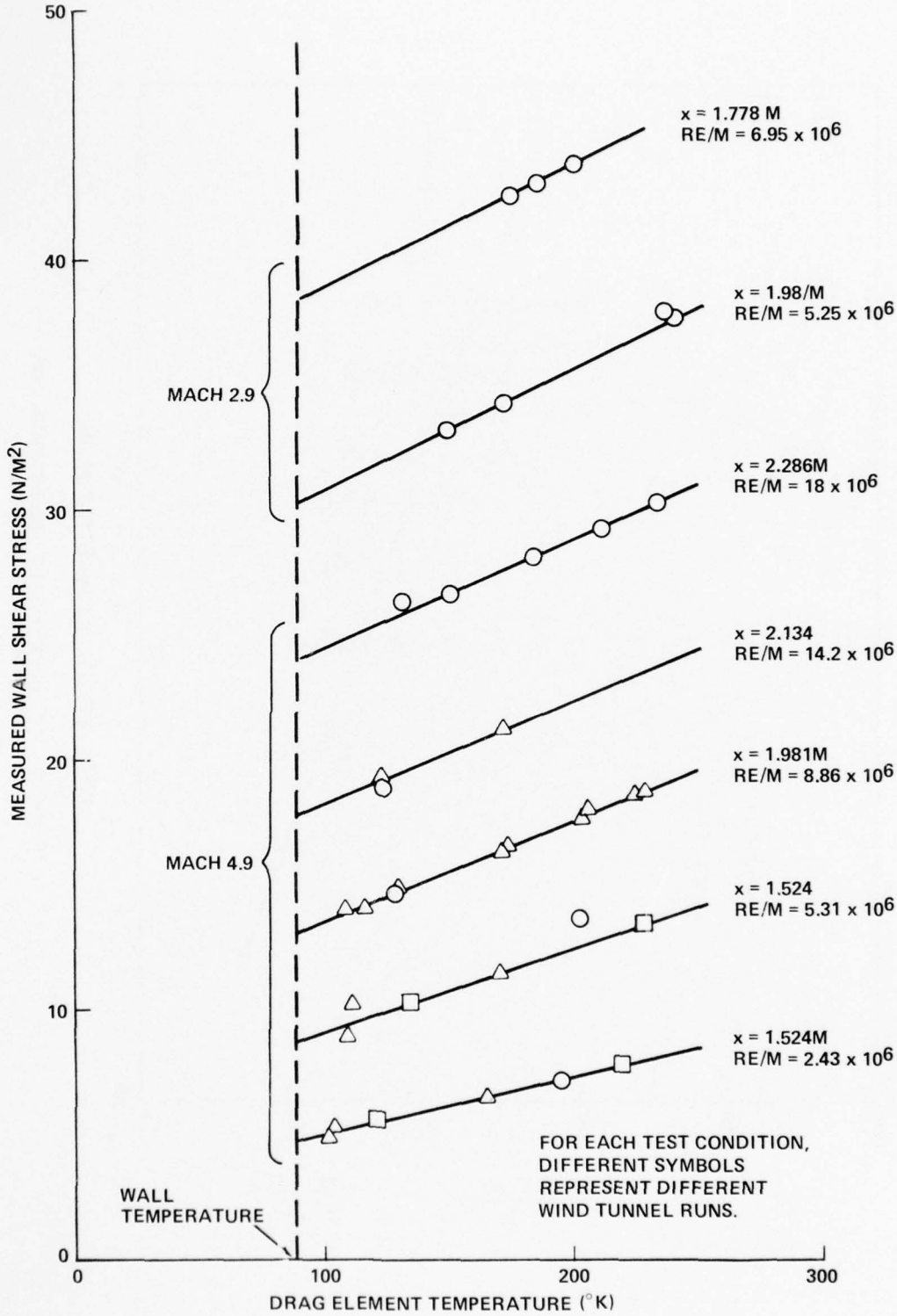

FIGURE 10 WALL SHEAR STRESS VARIATION WITH DRAG ELEMENT TEMPERATURE

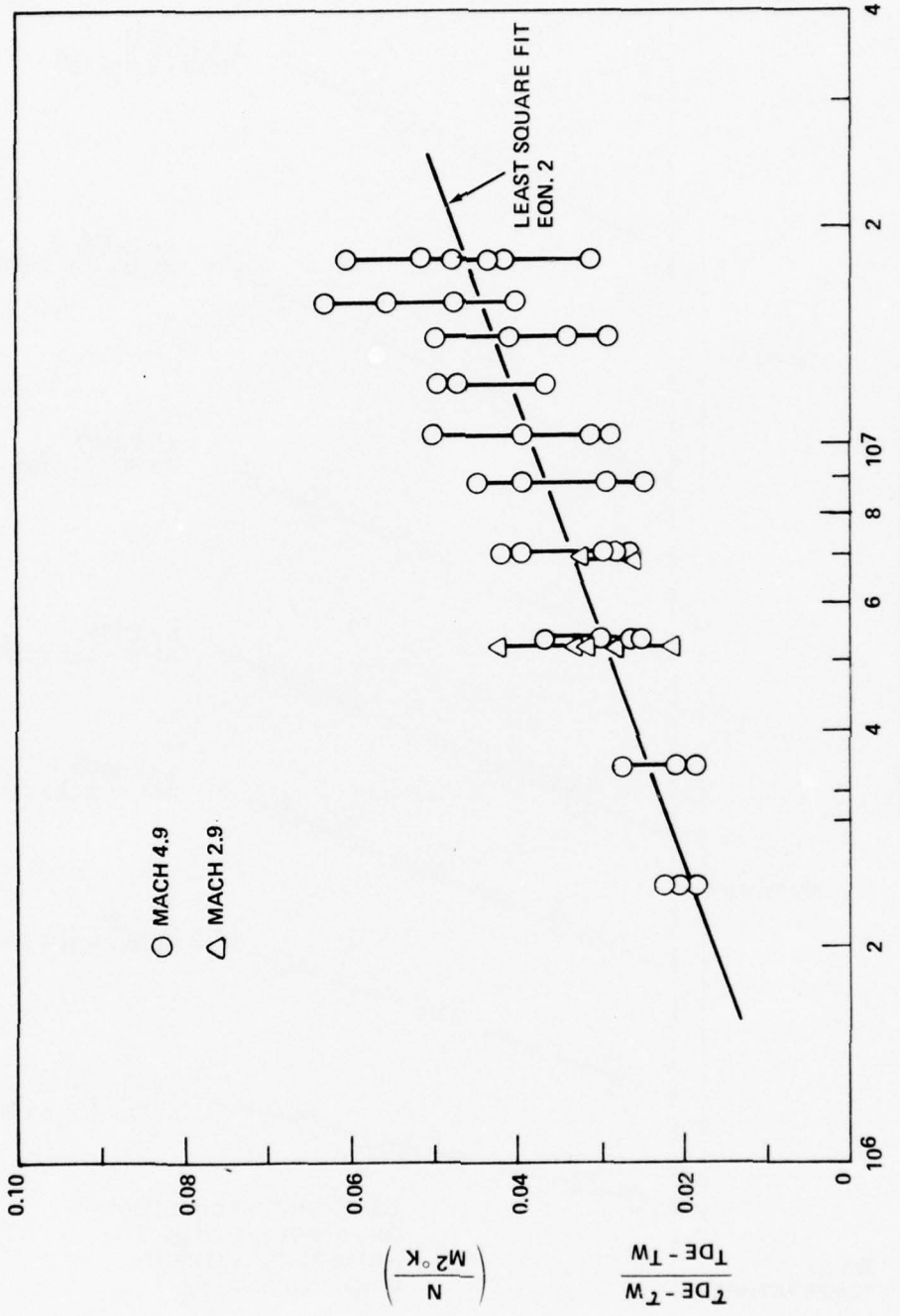

FIGURE 11 INFLUENCE OF REYNOLDS NUMBER ON TEMPERATURE STEP EFFECT.

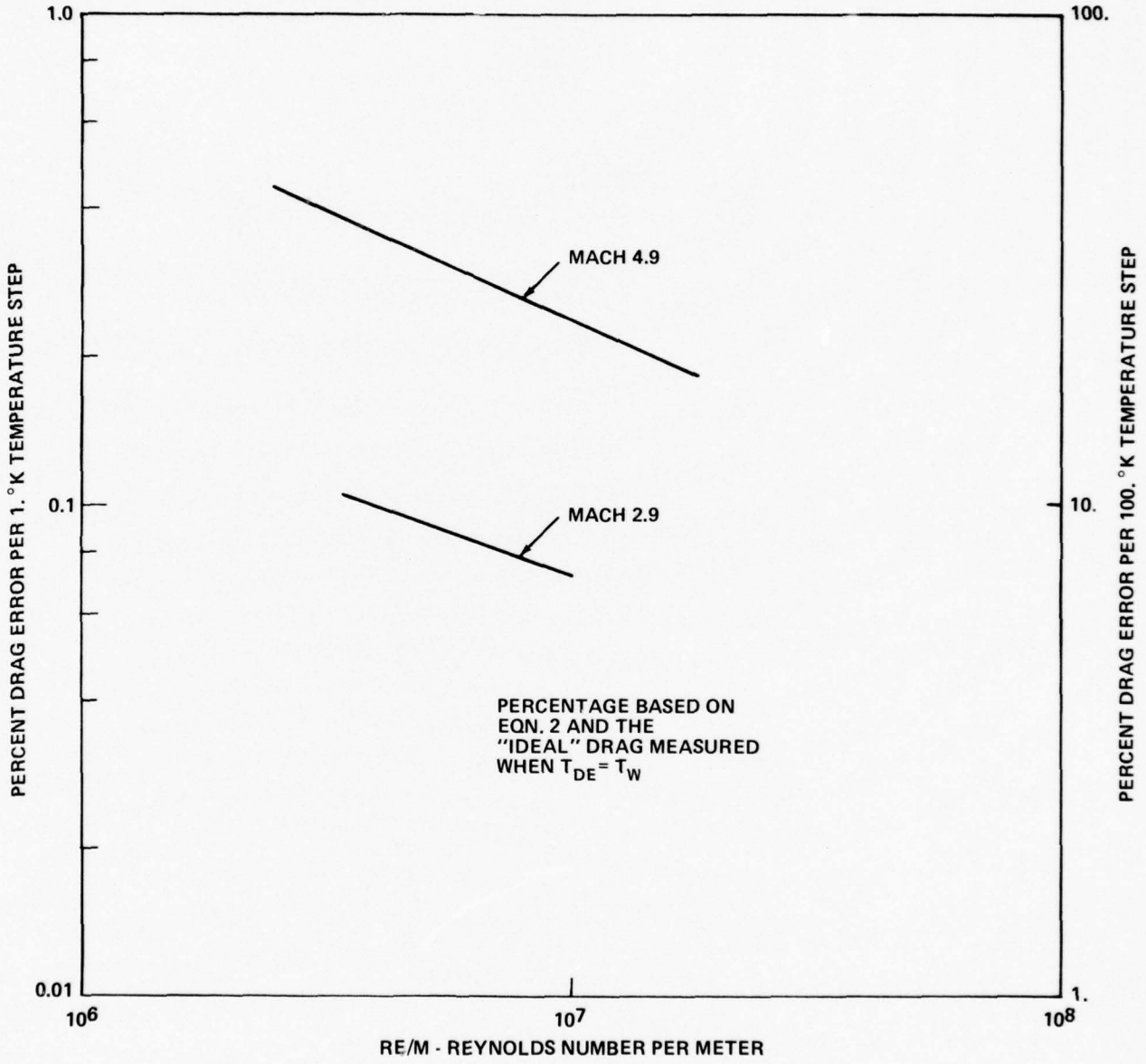

FIGURE 12 TEMPERATURE STEP EFFECTS IN PERCENT OF "IDEAL" DRAG.

APPENDIX A

CORRECTIONS TO PREVIOUSLY PUBLISHED DATA

In References 1 and 2 cold-wall skin-friction results were presented and a statement was made to the effect that the cold-wall data were obtained with a locally "hot" drag element. By applying the correction for temperature-step effects as derived in this study, significant changes to the previously published results are indicated.

Figure A1 shows a summary of the Mach 4.9 zero-pressure-gradient (ZPG) skin-friction data which was presented in Reference 1 together with corrected results. The data are shown in an incompressible frame of reference using the compressibility transformation of Van Driest (Reference A1) in the form:

$$\overline{C_f} = C_f \frac{r\,(0.2\,M_e^2)}{\left\{\sin^{-1}\left(\frac{2A^2 - B}{B^2 + 4A^2}\right) + \sin^{-1}\left(\frac{B}{\sqrt{B^2 + 4A^2}}\right)\right\}^2} \tag{A1}$$

$$\overline{R_{e_\theta}}' = \frac{\mu_e}{\mu_w} R_{e_\theta}' \tag{A2}$$

where:

$$A = \sqrt{\frac{T_e}{T_w} r\,0.2\,M_e^2} \qquad r = 0.89$$

$$B = \frac{T_{aw}}{T_w} - 1$$

Using this transformation, the effects of Mach number and heat transfer on the skin-friction coefficients are eliminated and the trends in the data are more easily noticed. Shown for comparison to the data is the incompressible, zero-pressure-gradient relation of Karman-Schroenherr (Reference A-2).

A1 Van Driest, E. R., "Turbulent Boundary Layer in Compressible Fluids," Journal of the Aeronautical Sciences, Vol. 18, No. 3, Mar 1951, pp. 145-160.

A2 Schoenherr, K. E., "Resistance of Flat Surfaces Moving Through a Fluid," Society of Naval Architects and Marine Engineers, Vol. 40, 1932, pp. 279-313.

Figure A1 shows the uncorrected cold-wall (CW) data of Reference 1 to have a trend which is quite different from the adiabatic-wall (AW) and moderate-heat-transfer (MHT) results. The AW and MHT skin-friction data are consistently (from 15 to 20 percent) below predicted values and vary inversely with the 0.25 power of Reynolds number. The higher skin-friction values and increased power relationship of the CW data could not be explained prior to the recent tests. Only when the temperature step correction, equation (2), is applied to the CW data do the CW results fall in line with the AW and MHT results. The values of CW skin-friction are reduced by the correction and the reduction is greater at the lower Reynolds numbers resulting in a change in the C_f vs. Re_θ power trend.

In a similar manner, the temperature-step correction was applied to the favorable-pressure-gradient (FPG) data of Reference 2. These results are shown in Figure A2. The trends of lower skin-friction values and reduced power exponent relationship with Reynolds number are again present, however, the magnitude of the correction is not as pronounced due to the higher values of wall shear stress which were experienced in the FPG flow field. Corrected tabulations of the ZPG and FPG data of References 1 and 2 are presented in Tables A1 and A2. These data listing should be considered as addendum to the previous data reports.

TABULAR OUTPUT NOMENCLATURE

The nomenclature used in the computerized tabular output (Tables A1 and A2) is defined as follows:

PO	tunnel supply pressure
TO	tunnel supply temperature
TW	wall temperature
TDE	drag-element temperature
MPW	Mach number
THP	boundary-layer momentum thickness
RTHPW	momentum thickness Reynolds number
TAUW(UNC)	wall shear stress (uncorrected)
TAUW(CORR)	wall shear stress (corrected)
CF	skin-friction coefficient (corrected)
BETADS	pressure-gradient parameter

BEST AVAILABLE COPY

TABLE A1 CORRECTED COLD-WALL SHEAR STRESS DATA OF REF. 1

PO N/M2	TO DEG.K	TW DEG.K	TDE DEG.K	MPW	THP CM	RTHPW	TAUW(UNC) N/M2	TAUW(CORR) N/M2	CF	BETADS
RUN NO. 110191, ZPG-CW, 1.524 M STATION, NOL BALANCE										
1.034E+06	426.7	90.0	201.7	4.968	.2771	4.718E+04	3.885E+01	3.379E+01	9.642E-04	0.000
9.308E+05	431.1	90.0	202.2	4.960	.2854	4.317E+04	3.642E+01	3.152E+01	9.92EE-04	0.000
8.274E+05	422.2	90.0	201.7	4.956	.2914	4.059E+04	3.369E+01	2.893E+01	1.022E-03	0.000
7.239E+05	424.4	90.0	201.1	4.961	.3022	3.644E+04	3.019E+01	2.568E+01	1.041E-03	0.000
6.205E+05	418.3	90.0	199.4	4.967	.3125	3.297E+04	2.660E+01	2.235E+01	1.062E-03	0.000
5.171E+05	422.2	90.0	197.2	4.961	.3281	2.850E+04	2.289E+01	1.901E+01	1.079E-03	0.000
4.137E+05	420.6	89.4	193.9	4.959	.3464	2.425E+04	1.921E+01	1.573E+01	1.114E-03	0.000
3.103E+05	421.1	88.9	190.0	4.937	.3717	1.966E+04	1.545E+01	1.246E+01	1.157E-03	0.000
2.068E+05	425.2	87.8	187.2	4.922	.4125	1.441E+04	1.131E+01	8.929E+00	1.229E-03	0.000
1.034E+05	423.3	87.8	178.3	4.871	.4874	8.769E+03	6.291E+00	4.936E+00	1.306E-03	0.000
RUN NO. 110181, ZPG-CW, 1.778 M STATION, NOL BALANCE										
1.034E+06	424.4	90.0	206.1	4.922	.2845	4.986E+04	3.864E+01	3.333E+01	9.173E-04	0.000
9.308E+05	425.6	90.0	204.4	4.917	.2927	4.606E+04	3.612E+01	3.106E+01	9.463E-04	0.000
8.274E+05	428.9	90.0	203.9	4.914	.3028	4.188E+04	3.299E+01	2.815E+01	9.627E-04	0.000
7.239E+05	421.1	90.0	202.8	4.916	.3112	3.877E+04	2.934E+01	2.471E+01	9.667E-04	0.000
6.205E+05	420.6	90.0	200.0	4.919	.3241	3.462E+04	2.606E+01	2.176E+01	9.963E-04	0.000
5.171E+05	424.4	90.0	197.2	4.919	.3413	2.954E+04	2.283E+01	1.893E+01	1.040E-03	0.000
4.137E+05	423.3	90.0	194.4	4.915	.3613	2.551E+04	1.909E+01	1.560E+01	1.068E-03	0.000
3.103E+05	423.3	88.9	191.7	4.899	.3890	2.074E+04	1.517E+01	1.213E+01	1.093E-03	0.000
2.068E+05	427.5	88.9	188.3	4.886	.4339	1.527E+04	1.113E+01	8.743E+00	1.171E-03	0.000
1.034E+05	421.1	87.8	181.7	4.836	.5143	9.476E+03	6.718E+00	5.282E+00	1.361E-03	0.000
RUN NO. 110141, ZPG-CW, 1.981 M STATION, NOL BALANCE										
1.034E+06	419.4	91.7	206.7	4.885	.2892	5.249E+04	3.639E+01	3.108E+01	8.314E-04	0.000
9.308E+05	426.1	91.7	205.6	4.902	.3003	4.747E+04	3.338E+01	2.833E+01	8.530E-04	0.000
8.274E+05	424.4	91.7	203.9	4.899	.3094	4.380E+04	3.098E+01	2.617E+01	8.849E-04	0.000
7.239E+05	423.3	91.1	201.7	4.902	.3205	3.982E+04	2.785E+01	2.331E+01	9.02BE-04	0.000
6.171E+05	421.7	90.6	198.9	4.895	.3339	3.568E+04	2.442E+01	2.019E+01	9.125E-04	0.000
5.171E+05	419.4	90.0	196.7	4.895	.3494	3.157E+04	2.092E+01	1.700E+01	9.166E-04	0.000
4.137E+05	422.2	88.9	192.8	4.891	.3721	2.666E+04	1.757E+01	1.408E+01	9.459E-04	0.000
3.103E+05	422.2	88.9	189.4	4.886	.4020	2.165E+04	1.417E+01	1.117E+01	9.970E-04	0.000
2.068E+05	418.3	88.9	184.4	4.874	.4462	1.635E+04	1.058E+01	8.233E+00	1.092E-03	0.000
1.034E+05	422.2	88.9	176.7	4.830	.5378	9.852E+03	6.320E+00	4.980E+00	1.277E-03	0.000
RUN NO. 110131, ZPG-CW, 2.134 M STATION, NOL BALANCE										
1.036E+06	418.9	91.7	204.4	4.861	.2924	5.382E+04	3.716E+01	3.192E+01	8.368E-04	0.000
9.308E+05	424.4	91.7	204.4	4.908	.3047	4.834E+04	3.457E+01	2.957E+01	8.945E-04	0.000
8.274E+05	420.6	91.1	203.3	4.906	.3135	4.491E+04	3.198E+01	2.716E+01	9.22BE-04	0.000
7.239E+05	424.4	90.6	201.1	4.903	.3266	4.039E+04	2.891E+01	2.438E+01	9.448E-04	0.000
6.205E+05	426.7	90.0	198.3	4.899	.3415	3.596E+04	2.554E+01	2.133E+01	9.617E-04	0.000
5.171E+05	422.2	89.4	194.4	4.895	.3574	3.195E+04	2.223E+01	1.838E+01	9.912E-04	0.000
4.137E+05	427.2	89.4	190.0	4.887	.3819	2.650E+04	1.876E+01	1.540E+01	1.031E-03	0.000
3.103E+05	427.8	88.9	185.0	4.866	.4130	2.157E+04	1.487E+01	1.202E+01	1.056E-03	0.000
2.068E+05	432.8	88.9	180.0	4.859	.4643	1.621E+04	1.107E+01	8.885E+00	1.165E-03	0.000
1.034E+05	412.8	88.9	171.1	4.794	.5470	1.060E+04	7.206E+00	5.893E+00	1.469E-03	0.000
RUN NO. 110151, ZPG-CW, 2.286 M STATION, NOL BALANCE										
1.034E+06	426.7	91.7	212.8	4.823	.2989	5.424E+04	3.783E+01	3.223E+01	8.215E-04	0.000
9.308E+05	431.1	91.7	209.4	4.876	.3114	4.888E+04	3.457E+01	2.936E+01	8.664E-04	0.000
8.274E+05	422.2	91.7	206.7	4.868	.3186	4.612E+04	3.093E+01	2.597E+01	8.570E-04	0.000
7.239E+05	423.3	91.7	203.9	4.849	.3305	4.204E+04	2.785E+01	2.321E+01	8.624E-04	0.000
6.205E+05	421.7	91.1	200.6	4.857	.3450	3.771E+04	2.478E+01	2.047E+01	8.931E-04	0.000
5.171E+05	418.3	90.0	196.7	4.846	.3615	3.351E+04	2.137E+01	1.742E+01	9.041E-04	0.000
4.137E+05	418.3	88.9	192.8	4.846	.3851	2.856E+04	1.766E+01	1.412E+01	9.163E-04	0.000
3.103E+05	422.2	88.9	188.9	4.837	.4190	2.306E+04	1.405E+01	1.104E+01	9.481E-04	0.000
2.068E+05	422.2	88.9	183.9	4.820	.4691	1.733E+04	1.025E+01	7.901E+00	1.005E-03	0.000
1.034E+05	422.2	88.9	177.2	4.818	.5706	1.056E+04	6.263E+00	4.907E+00	1.246E-03	0.000

BEST AVAILABLE COPY

TABLE A2 CORRECTED COLD-WALL SHEAR STRESS DATA OF REF. 2

PO N/M2	TO DEG.K	TW DEG.K	TDE DEG.K	RRW	THP CM	RTHRW	TAUW(UNC) N/M2	TAUW(CORR) N/M2	CF	BETACS
RUN NO. 202071, FPG-CW= 1.270 M STATION, NOL BALANCE										
1.032E+06	420.8	97.2	223.9	4.021	.1783	4.819E+04	9.495E+01	8.842E+01	1.181E-03	-.797
9.280E+05	423.3	97.8	227.2	4.006	.1830	4.440E+04	8.808E+01	8.159E+01	1.197E-03	-.789
8.274E+05	430.7	98.9	229.4	4.016	.1895	3.973E+04	8.255E+01	7.626E+01	1.266E-03	-.769
7.226E+05	427.8	97.8	229.4	4.015	.1953	3.615E+04	7.516E+01	6.904E+01	1.311E-03	-.755
6.219E+05	429.1	96.7	228.9	4.013	.2026	3.216E+04	6.753E+01	6.166E+01	1.358E-03	-.745
5.178E+05	422.2	96.7	226.1	4.017	.2106	2.846E+04	5.917E+01	5.370E+01	1.426E-03	-.729
4.116E+05	422.8	96.7	222.8	3.997	.2221	2.405E+04	5.056E+01	4.562E+01	1.499E-03	-.704
3.103E+05	425.6	95.6	216.7	3.996	.2382	1.927E+04	4.077E+01	3.650E+01	1.590E-03	-.692
2.068E+05	426.1	92.2	211.1	3.994	.2627	1.415E+04	3.016E+01	2.662E+01	1.736E-03	-.671
1.027E+05	417.8	87.8	200.6	3.949	.3069	8.654E+03	1.733E+01	1.496E+01	1.892E-03	-.652
RUN NO. 202031, FPG-CW= 1.778 M STATION, NOL BALANCE										
1.034E+06	426.1	112.2	227.8	4.423	.2330	5.086E+04	5.762E+01	5.199E+01	9.649E-04	-.762
9.284E+05	427.6	127.8	230.0	4.421	.2395	4.680E+04	5.260E+01	4.778E+01	9.845E-04	-.751
8.274E+05	423.3	117.8	231.1	4.423	.2455	4.333E+04	4.886E+01	4.367E+01	1.013E-03	-.737
7.205E+05	424.0	102.2	228.9	4.418	.2540	3.905E+04	4.475E+01	3.919E+01	1.039E-03	-.723
6.178E+05	422.2	138.9	227.2	4.415	.2633	3.457E+04	3.779E+01	3.408E+01	1.052E-03	-.720
5.171E+05	421.1	138.9	227.2	4.405	.2745	3.079E+04	3.265E+01	2.915E+01	1.066E-03	-.714
4.130E+05	422.9	105.6	222.8	4.409	.2907	2.582E+04	2.937E+01	2.509E+01	1.152E-03	-.674
3.096E+05	425.0	92.2	211.7	4.492	.3156	2.006E+04	2.417E+01	2.035E+01	1.333E-03	-.638
2.068E+05	426.1	91.7	203.3	4.372	.3440	1.540E+04	1.766E+01	1.462E+01	1.301E-03	-.609
1.034E+05	427.8	91.7	190.0	4.342	.4071	9.191E+03	1.052E+01	8.746E+00	1.520E-03	-.536
RUN NO. 202021, FPG-CW= 1.981 M STATION, NOL BALANCE										
1.034E+06	427.2	92.2	224.4	4.553	.2529	5.177E+04	5.439E+01	4.807E+01	9.898E-04	-.680
9.287E+05	427.8	94.4	222.8	4.540	.2595	4.789E+04	5.114E+01	4.518E+01	1.025E-03	-.663
8.274E+05	417.8	93.3	217.8	4.536	.2645	4.522E+04	4.780E+01	4.215E+01	1.070E-03	-.627
7.267E+05	424.4	94.4	215.6	4.550	.2753	4.007E+04	4.326E+01	3.803E+01	1.112E-03	-.616
6.205E+05	419.4	93.3	213.3	4.535	.2846	3.628E+04	3.797E+01	3.300E+01	1.116E-03	-.610
5.171E+05	423.3	92.2	208.9	4.531	.2988	3.134E+04	3.335E+01	2.883E+01	1.166E-03	-.589
4.102E+05	425.6	92.2	204.4	4.510	.3164	2.637E+04	2.770E+01	2.369E+01	1.189E-03	-.576
3.096E+05	424.2	92.2	200.0	4.517	.3393	2.138E+04	2.140E+01	1.797E+01	1.201E-03	-.583
2.062E+05	423.6	91.7	195.6	4.491	.3742	1.592E+04	1.566E+01	1.290E+01	1.268E-03	-.553
1.034E+05	418.9	91.7	188.3	4.471	.4415	9.684E+03	9.091E+00	7.385E+00	1.424E-03	-.503
RUN NO. 202011, FPG-CW= 2.134 M STATION, NOL BALANCE										
1.034E+06	430.6	97.2	197.8	4.624	.2672	5.230E+04	5.296E+01	4.822E+01	1.051E-03	-.521
9.294E+05	422.2	97.2	202.8	4.622	.2724	4.944E+04	5.014E+01	4.526E+01	1.096E-03	-.501
8.274E+05	423.3	96.1	203.3	4.624	.2809	4.517E+04	4.640E+01	4.162E+01	1.133E-03	-.488
7.226E+05	424.2	94.4	203.3	4.622	.2908	4.074E+04	4.202E+01	3.737E+01	1.164E-03	-.478
6.178E+05	426.9	94.4	202.8	4.614	.3031	3.607E+04	3.715E+01	3.277E+01	1.186E-03	-.469
5.178E+05	424.4	93.3	200.6	4.621	.3165	3.176E+04	3.275E+01	2.865E+01	1.244E-03	-.454
4.158E+05	425.0	91.7	196.7	4.602	.3340	2.710E+04	2.761E+01	2.390E+01	1.273E-03	-.441
3.103E+05	423.9	91.7	190.6	4.600	.3593	2.185E+04	2.137E+01	1.827E+01	1.302E-03	-.437
2.062E+05	422.2	91.7	184.4	4.578	.3968	1.631E+04	1.590E+01	1.348E+01	1.420E-03	-.401
1.020E+05	421.7	91.7	175.0	4.545	.4722	9.770E+03	9.547E+00	8.142E+00	1.685E-03	-.340

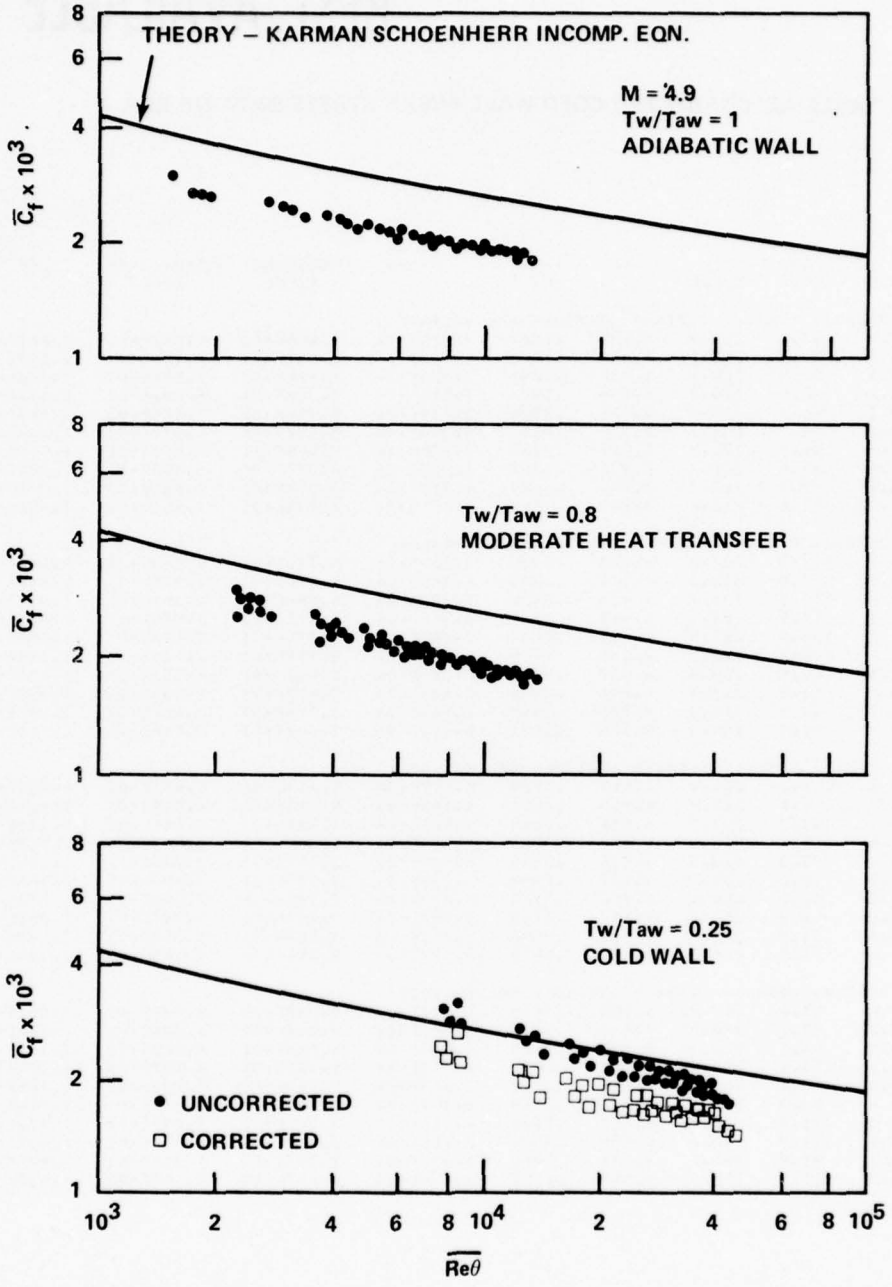

FIGURE A1 INFLUENCE OF TEMPERATURE STEP CORRECTION ON THE DATA OF REF. 1

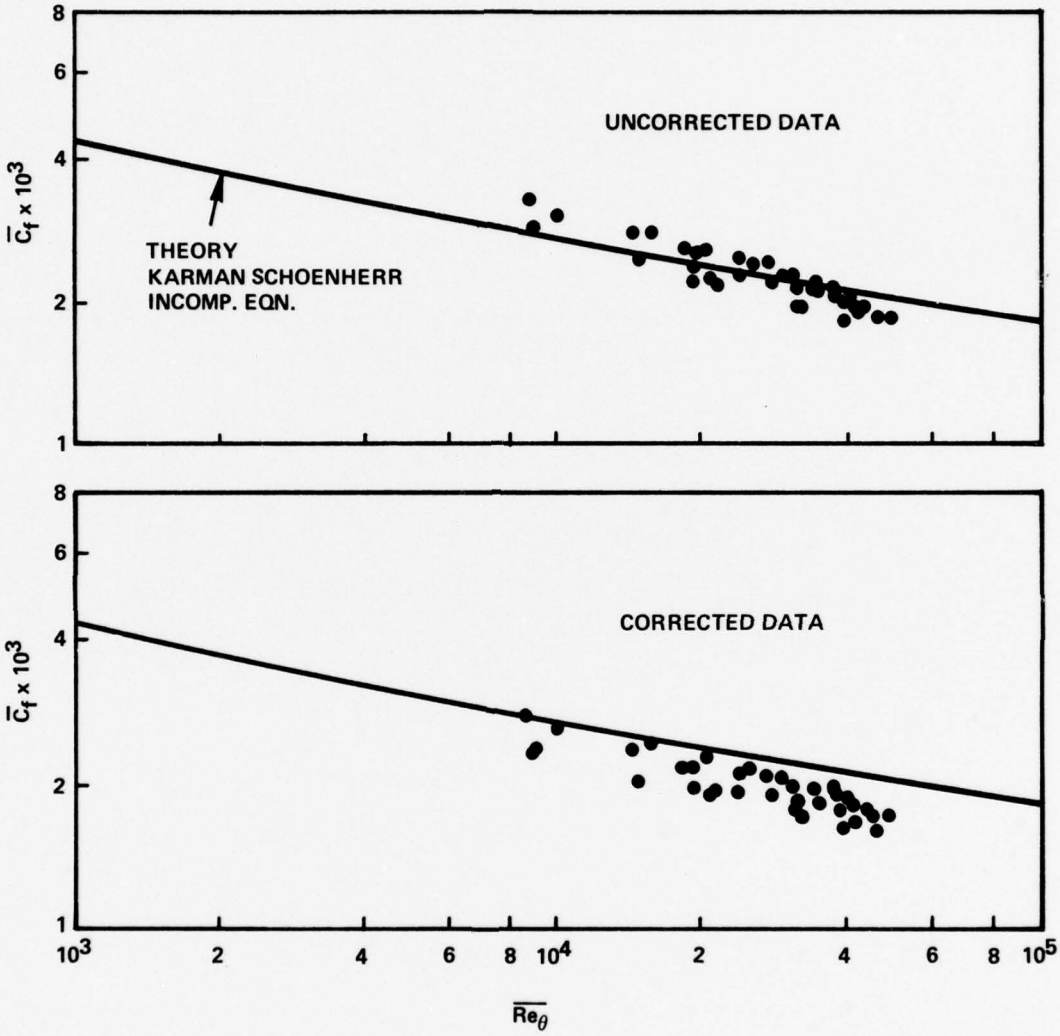

FIGURE A2 INFLUENCE OF TEMPERATURE STEP CORRECTION ON THE CW DATA OF REF. 2

DISTRIBUTION

Copies

NAVY

Commander
Naval Sea Systems
Command Headquarters
Attn: SEA-03B 1
SEA-035 1
SEA-09G32 2
SEA-03513
Department of the Navy
Washington, DC 20362

Commander
Naval Air Systems Command
Headquarters
Attn: AIR 03B 1
AIR 03E 1
AIR 03P2 1
AIR 320 1
AIR 320C 1
AIR 5301 1
AIR 310 1
AIR 954 2
Department of the Navy
Washington, DC 20361

Chief of Naval Research
Attn: Mr. Morton Cooper
Code 430B 1
Technical Library 1
800 North Quincy Street
Arlington, VA 22217

Commander
David W. Taylor Naval Ship
Research and Development
Center
Attn: Aerodynamics Library
(522.3) 1
Bethesda, MD 20084

Copies

Commander
Naval Weapons Center
Attn: Technical Library
(Code 753) 1
R. W. Van Aken
(Code 316) 1
China Lake, CA 93555

Commanding Officer
Naval Research Laboratory
Attn: Library (2620) 2
Washington, D. C. 20375

Commander
Pacific Missile Test Center
Attn: Technical Library 1
Point Mugu, CA 93042

Director
Strategic Systems Project
Office
Attn: NSP-2722 1
NSP-43 1
Department of the Navy
Washington, DC 20376

Commander
Naval Air Development
Center
Attn: Code 8131 1
Warminster, PA 18974

Superintendent
Naval Postgraduate School
Monterey, CA 95076 1

DISTRIBUTION (CONT)

Copies

Superintendent
U.S. Naval Academy
Attn: Director of Research
Nimitz Library 1
Annapolis, MD 21402

Commander
Naval Material Command
Attn: MAT 08T1 1
MAT 08T2 1
MAT 08T22 1
Washington, DC 20360

Commanding Officer
Naval Ordnance Station
Attn: Technical Library 1
Indian Head, MD 20640

ARMY

Army Material Command
(Hdqtrs)
Attn: Technical Library 1
5001 Eisenhower Avenue
Alexandria, VA 22333

Director
USA Ballistic Research
Laboratories
Attn: DRDAR-TSB (Technical
Library Division) 1
DRXBL-LF 1
Aberdeen Proving Ground, MD 21005

Commanding Officer
Harry Diamond Laboratories
Attn: Scientific and
Technical Information
Office 1
2800 Powder Mill Road
Adelphi, MD 20783

Copies

Commander
U. S. Army Missile Research
and Development Command
Attn: DRDMI-TB Scientific
Information
Center 1
Mr. R. A. Deep,
DRDMI-TDK 1
Redstone Arsenal, AL 35809

U. S. Army Ballistic Missile
Defense Agency
Attn: Dr. Sidney Alexander 1
1100 Commonwealth Building
1320 Wilson Boulevard
Arlington, VA 22209

Commander
U. S. Army Armament
Research and Development
Command
Attn: Mr. A. A. Loeb
DRDAR-LCA-FB 1
Picatinny Arsenal
Dover, NJ 07801

Commander
U. S. Army ARRADCOM
Attn: DRDAR-ACW 1
Aberdeen Proving
Ground, MD 21005

Commander
U. S. Army Research Office
Attn: DRXRO (Technical
Library) 1
P. O. Box 12211
Research Triangle
Park, NC 27709

Director
Ballistic Missile Defense
Advanced Technology
Center 1
Attn: Technical Library 1
P. O. Box 1500
Huntsville, AL 35807

DISTRIBUTION (CONT)

Copies

AIR FORCE

Air Force
Office of Scientific Research
Library (AFOSE Library)
1400 Wilson Blvd.
Arlington, VA 22209 1

Air Force
Systems Command Headquarters
Library (DPSL)
Andrews Air Force
Base, MD 20334 1

Commander
Space and Missile Systems
Organization
Attn: Technical Library 1
Los Angeles Air Force
Station
P. O. Box 92960
World Way Postal
Center, CA 90009

Headquarters
Arnold Engineering
Development Center
Attn: Arnold Center,
Library 2
Arnold Air Force
Station, TN 37389

von Karman Gas Dynamics
Facility
Sverdrup/ARL, Incorporated
Arnold Air Force
Station, TN 37388

Department of Aeronautics
DFAN
USAF Academy, CO 80840 1

Copies

Commanding Officer
U. S. Air Force Weapons
Laboratory
Attn: WLRP 1
Dr. J. Walsh 1
Technical Library (SUL)
Kirtland Air Force Base
Albuquerque, NM 87117

Air Force Systems Command
Air Force Flight Dynamics
Laboratory
Attn: Aeromechanics Division
(FX) 1
Technical Library 1
Wright Patterson Air Force
Base, OH 45433

Air Force Armament Test
Laboratory
Attn: C. Butler (DLM1) 1
Technical Library 1
Eglin Air Force
Base, FL 32542

NASA

Ames Research Center
National Armament and Space
Administration
Attn: Technical Information
Division (AT) 1
Moffett Field, CA 94035

Langley Research Center
National Aeronautics and
Space Administration
Attn: Technical Library
Braner (4230,
MS 185) 1
Langley Station
Hampton, VA 23665

DISTRIBUTION (CONT)

	Copies
Lewis Research Center National Aeronautics and Space Administration Attn: Library - Mail Stop 60-3	1
Library Branch (1950, MS 60-3)	1
21000 Brookpark Road Cleveland, OH 44135	
George C. Marshall Space Flight Center National Aeronautics and Space Administration Attn: Central Library	1
Redstone Scientific Information Center	1
Marshall Space Flight Center, AL 35812	
National Aeronautics and Space Administration Attn: Technical Library (KSS-10)	1
Washington, DC 20546	
OTHER FEDERAL GOVERNMENT	
National Bureau of Standards Library E01 Administration Bldg. Washington, DC 20234	1
Los Alamos Scientific Laboratory Attn: Report Library	1
P. O. Box 1663 Los Alamos, NM 87544	
Defense Documentation Center Cameron Station Alexandria, VA 22314	12
Defense Nuclear Agency Attn: Technical Library Washington, DC 20305	1
Defense Advanced Research Projects Agency Attn: Technical Library 1400 Wilson Blvd. Arlington, VA 22209	1
UNIVERSITY	
Aerospace Engineering Program Attn: Prof. W. K. Rey, Chrm.	1
University of Alabama P. O. Box 6307 University, AL 35486	
AME Department University of Arizona Attn: Dr. L. B. Scott, Jr.	1
Tucson, AZ 85719	
Brown University Division of Engineering Attn: Dr. M. Sibulkin	1
Library	1
Division of Engineering Providence, RI 02912	
California Institute of Technology Attn: Graduate Aeronautical Laboratories Library	1
Dr. H. W. Liepmann Karman Lab-301	1
Prof. L. Lees, Firestone Flight Science Lab.	1
Dr. D. E. Coles, 306 Karman Lab.	1
Dr. A. Roshko	1
Pasadena, CA 91109	

DISTRIBUTION (CONT)

Copies

Dr. John D. Nicolaides, Head
Aero Engineering Dept.
California State Polytechnic University
San Luis Obispo, CA 93401 1

University of California
Attn: Dr. M. Holt,
Dr. A. K. Oppenheim,
Div. of Aeronautical Sciences 1
Berkeley, CA 94720

Department of Aerospace Engineering
Attn: Dr. John Laufer 1
University of Southern California
University Park
Los Angeles, CA 90007

University of California - San Diego
Department of Aerospace and Mechanical Engineering Sciences
Attn: Dr. P. A. Libby 1
LaJolla, CA 92037

Case Western Reserve University
Attn: Dr. E. Reshotko 1
3306 Clarendon Road
Cleveland, OH 44118

The Catholic University of America
Attn: Dr. C. C. Chang 1
Dr. Paul K. Chang
Mechanical Engr. Dept. 1
Dr. M. J. Casarella
Mechanical Engr. Dept. 1
Washington, DC 20017

Copies

University of Cincinnati
Attn: Department of Aerospace Engineering 1
Dr. Arnold Polak 1
Cincinnati, OH 45221

Department of Aerospace Engineering Sciences
University of Colorado
Boulder, CO 80301 1

Cornell University
Graduate School of Aero. Engineering
Attn: Dr. S. F. Shen 1
Prof. F. K. Moore 1
Ithaca, NY 14850

University of Delaware
Mechanical and Aeronautical Engineering Dept
Attn: Dr. James E. Danberg 1
Newark, DE 19711

George Washington University
Attn: Library 1
2130 H. Street N.W.
Washington, DC 20052

Georgia Institute of Technology
Attn: Dr. Arnold L. Ducoffe
Aerospace Engineering Dept. 1
225 North Avenue, N.W.
Atlanta, GA 30332

Technical Reports Collection
Gordon Mckay Library
Harvard University
Div. of Eng'g. and Applied Physics
Pierce Hall, Oxford Street
Cambridge, MA 02138

DISTRIBUTION (CONT)

	Copies
Illinois Institute of Technology	
Attn: Dr. M. V. Morkovin	1
Prof. A. A. Fejer, M.A.E. Dept.	1
3300 South Federal	
Chicago, IL 60616	
University of Illinois	
Attn: Aeronautical and Astronautical Engineering Department	1
101 Transportation Bldg.	
Urbana, IL 61801	
Iowa State University	
Attn: Aerospace Engineering Department	1
Ames, IA 50010	
The Johns Hopkins University	
Mechanics Department	
Attn: Prof. S. Corrsin	1
Baltimore, MD 21218	
University of Kentucky	
Wenner-Gren Aero. Lab.	
Lexington, KY 40506	
Department of Aero. Engineering ME 106	
Louisiana State University	
Attn: Dr. P. H. Miller	1
Baton Rouge, LA 70803	

	Copies
University of Maryland	
Attn: Prof. A. Wiley Sherwood Department of Aerospace Engineering	1
Dr. S. I. Pai, Institute of Fluid Dynamics and Applied Mathematics	1
Dr. Redfield W. Allen Department of Mechanical Engineering	1
Dr. W. L. Melnik Department of Aerospace Engr.	1
Dr. John D. Anderson, Jr. Department of Aerospace Engineering	1
Engineering and Physical Sciences Library	1
College Park, MD 20742	
Massachusetts Institute of Technology	
Attn: Prof. J. Baron, Dept. of Aero. and Astro., Rm. 37-461	1
Prof. A. H. Shapiro, Institute Professor	1
Aero. Engineering Library	1
Prof. Ronald F. Probestein	1
Dr. E. E. Covert Aerophysics Laboratory	1
Cambridge, MA 02139	

DISTRIBUTION (CONT)

	Copies
Michigan State University Library Attn: Documents Department East Lansing, MI 48823	1
University of Michigan Attn: Dr. M. Sichel, R. M. Howe, Dept. of Aero. Engineering	1
Engineering Library	1
Aerospace Engineering Library Aquisitions Section Serials Division Ann Arbor, MI 48105	1
Mississippi State University Department of Aerophysics and Aerospace Engineering P. O. Drawer A State College, MI 39762	
U. S. Naval Academy Attn: Engineering Department, Aerospace Division Annapolis, MD 21402	1
Library, Code 2124 U. S. Naval Postgraduate School Attn: Technical Reports Section Monterey, CA 93940	1
New York University Aerospace and Energetics Lab Attn: Prof. V. Zakkay	1
Engineering and Science Library Merrick and Stewart Aves. Westbury, L.I., NY 11590	1
North Carolina State University Attn: Dr. H. A. Hassan, Dept. of Mech. and Aero. Engineering Raleigh, NC 27607	1
D. H. Hill Library North Carolina State University P. O. Box 5007 Raleigh, NC 27607	
Northwestern University Technological Institute Attn: Department of Mechanical Engineering	1
Library Evanston, IL 60201	1
Ohio State University Attn: Aero. Civil Library	1
Prof. J. D. Lee, Aeronautical Research Lab.	1
Prof. G. L. Von Eschen, Dept. of Aero-Astro Engineering 2036 Neil Avenue Columbus, OH 43210	1
Ohio State University Libraries Documents Division 1858 Neil Avenue Columbus, OH 43210	
Oklahoma State University Office of Engineering Research Stillwater, OK 74074	

DISTRIBUTION (CONT)

Copies

Department of Aerospace Engineering
Room 233 Hammond Building
The Pennsylvania State University
University Park, PA 16802

Pennsylvania State University Library
Documents Section
University Park, PA 16802

Polytechnic Institute of New York
Graduate Center Library
Attn: Dr. R. J. Cresci 1
Route 11
Farmingdale, L.I., NY 11735

Polytechnic Institute of New York
Attn: Reference Department 1
Spicer Library
333 Jay Street
Brooklyn,NY 11201

Bevier Engineering Library
Attn: Librarian 1
126 Benedum Hall
University of Pittsburgh
Pittsburgh, PA 15213

Princeton University
James Forrestal Research Center
Attn: Prof. S. Bogdonoff
Gas Dynamics Laboratory
Princeton, NJ 08540

Copies

Purdue University
School of Aeronautical and Engineering Sciences
Attn: Library 1
Dr. P. S. Lykoudis, Dept. of Aero. Engineering 1
Lafayette, IN 47901

Rensselaer Polytechnic Institute
Attn: Dept. of Aeronautical Engineering and Astronautics 1
Dr. Robert E. Duffy 1
Troy, NY 12181

Rutgers - The State University
Attn: Dr. R. H. Page, Dept. of Mech. and Aero. Engineering 2
University Heights Campus
New Brunswick, NJ 08903

Stanford University
Attn: Librarian, Dept. of Aeronautics and Astronautics 1
Stanford, CA 94305

Stevens Institute of Technology
Attn: Mechanical Engineering Department 1
Library 1
Hoboken, NJ 07030

The University of Texas at Austin
Attn: Director 1
Applied Research Laboratories
P. O. Box 8029
Austin, TX 78712

DISTRIBUTION (CONT)

	Copies
University of Toledo Department of Aero. Engineering Research Foundation Toledo, OH 43606	
Documents Department Virginia Polytechnic Institute and State University Attn: Carol M. Newman Library Blacksburg, VA 24061	1
University of Virginia Attn: Alderman Library Science Reference Division Charlottesville, VA 22901	1
University of Washington Attn: Engineering Library	1
Department of Aeronautics and Astronautics	1
Prof. R. E. Street, Dept. of Aero. and Astro.	1
Prof. A. Hertzberg, Aero. and Astro. Guggenheim Hall Seattle, WA 98105	1
West Virginia University Attn: Library Morgantown, WV 26506	1
Federal Reports Center University of Wisconsin 462 Mechanical Engineering Building 1513 University Avenue Madison, WI 53706	1

	Copies
INDUSTRY	
Acurex Corporation Attn: Dr. L. J. Alpinieri 485 Clyde Avenue Mountain View, CA 94040	1
Aeroneutronic Ford Corporation Aeroneutronic Division Attn: Dr. A. Demetriades Newport Beach, CA 92660	1
Aeronautical Research Associates of Princeton Attn: Dr. C. duP. Donaldson 50 Washington Road Princeton, NJ 08540	1
AVCO-Everett Research Laboratory Attn: Library	1
Dr. George Sutton 2385 Revere Beach Parkway Everett, MA 02149	1
AVCO Systems Division, AVCO Corporation Attn: E. E. H. Schurmann	1
V. D. Cristina	1
N. A. Thyson 201 Lowell Street Wilmington, MA 01887	1
Fairchild Republic Co. Fairchild Industries, Inc. Attn: Engineering Library Farmingdale, NY 11735	1

DISTRIBUTION (CONT)

Copies

CONVAIR Division, General Dynamics Corporation
Library and Information Services
P. O. Box 80877
San Diego, CA 92138

CONVAIR Division
General Dynamics Corporation
Attn: Research Library 2246 1
P. O. Box 748
Fort Worth, TX 76101

General Dynamics Corporation
Pomona Division
Attn: Division Library Mail Zone 6-20 1
Pomona, CA 91766

General Electric Company
AEG Technical Information Center N-32
Cincinnati, OH 45215

General Electric Company
Missile and Space Division
Attn: MSD Library 1
Larry Chasen, Mgr. 1
Dr. J. D. Stewart, Mgr. Research and Engineering 1
Dr. S. M. Scala 1
Dr. H. Lew 1
Mr. J. W. Faust 1
Mr. W. Daskin 1
S. B. Kottock 1
L. A. Marshall 1
A. Martellucci 1
P. O. Box 8555
Philadelphia, PA 19101

Copies

General Electric Research and Development Center
The Whitney Library
The Knolls, K-1
P. O. Box 8
Schenectady, NY 12301

General Research Corporation
Attn: Technical Info. Officer 1
5383 Hollister Avenue
P. O. Box 3587
Santa Barbara, CA 93105

Grumman Aerospace Corporation
Attn: Dr. R. A. Scheuing 1
Mr. H. B. Hopkins 1
Bethpage, L.I., NY 11714

HERCULES Incorporated
Allegany Ballistics Laboratory
Attn: Mrs. Louise E. Derrick Librarian 1
P. O. Box 210
Cumberland, MD 21502

Hughes Aircraft Company
Attn: Co. Tech. Doc. Ctr., MS 6/E110 1
Continela and teale Streets
Culver City, CA 90230

Institute for Defense Analyses
Attn: Classified Library 1
400 Army-Navy Drive
Arlington, VA 22202

Kaman Nuclear
1700 Garden of the Gods Road
Colorado Springs, CO 80907

DISTRIBUTION (CONT)

Copies

Kaman Science Corporation
Avidyne Division
Attn: Dr. J. R. Ruetenik
83 Second Avenue
Burlington, MA 01803

Lockheed Aircraft Corporation
Vice President and Chief Scientist Dept. 03-01
Attn: Dr. Ronald Smelt 1
P. O. Box 551
Burbank, CA 91520

Lockheed-California Company
Attn: Central Library
Dept. 84-40
Bldg. 170,
PLT. B-1 1
Burbank, CA 91502

Lockheed Missiles and Space Company
Attn: Technical Information Center 1
Dr. R. P. Caren 1
3251 Hanover Street
Palo Alto, CA 94304

Lockheed Missiles and Space Company
Lockheed Aircraft Corporation
Attn: G. T. Chrusciel 1
Dr. L. E. Ericson 1
L. Hull 1
J. P. Reding 1
L. Lee 1
P. O. Box 504
Sunnyvale, CA 94088

Copies

Martin Marietta Corporation
Attn: Science-Technology Library (Mail No. 398) 1
P. O. Box 988
Baltimore, MD 21203

Martin Marietta Corporation
Orlando Division
Attn: Technical Library 1
Sandlake Road
Orlando, FL 32805

M.I.T. Lincoln Laboratory
Attn: Library A-082 1
Dr. S. Edelberg 1
P. O. Box 73
Lexington, MA 02173

McDonnell Aircraft Company
McDonnell Douglas Corporation
Research and Engineering Library
Dept. 209, Bldg. 33
P. O. 516
St. Louis, MI 63166 1

McDonnell Douglas Astronautics Company
Space Systems Center
Attn: A2-260 Library 1
Dr. J. S. Murphy, A-830 1
Mr. W. H. Branch, Director 1
A3-339 Library 1
5301 Bolsa Avenue
Huntington Beach, CA 92647

DISTRIBUTION (CONT)

	Copies
Nielson Engineering and Research, Incorporated Attn: Dr. J. N. Nielson 510 Clyde Avenue Mountain View, CA 94043	1
Northrop Corporation Attn: Technical Info. 3343-32 3901 West Broadway Hawthorne, CA 90250	1
Raytheon Company Missile Systems Division Attn: H. H. Roscoe Hartwell Road Bedford, MA 01730	1
Columbus Aircraft Division Rockwell International Corporation Engineering Data Services 4300 E. Fifth Avenue Columbus, OH 43216	1
Rockwell International B-1 Division Attn: LAD Library, Dept. 299 International Airport Technical Information Center (BA08) Los Angeles, CA 90009	1
Sandia Laboratories Attn: Mr. K. Goin, 5217	1
Mrs. B. R. Allen Div 3421	1
Mr. R. Maydew	1
Mr. D. McBride Albuquerque, NM 87115	1
Science Application, Incorporated Missile Technology Division Attn: L. A. Cassel 201 West Dyer Road, Unit B Santa Anna, CA 92707	1
Stanford Research Institute Attn: Library 333 Ravenswood Avenue Menlo Park, CA 94025	1
The Aerospace Corporation Attn: Dr. W. R. Warren, Jr. 130/691 2350 E. El Sequnda Blvd. El Segunda, CA 90245	1
The Boeing Company Attn: Aerospace Library 8K-38	
J. M. MacDonald P. O. Box 3999 Seattle, WA 98124	1
The Johns Hopkins University Applied Physics Laboratory Attn: Document Library	1
Dr. F. K. Hill	1
Dr. L. L. Cronvich Johns Hopkins Road Laurel, MD 20810	1
The RAND Corporation Attn: Library - D 1700 Main Street Santa Monica, CA 90406	1
TRW Incorporated Attn: Technical Library-Document Acquisitions 1 Space Park Redondo Beach, CA 90278	1

DISTRIBUTION (CONT)

	Copies	Copies
United Technologies Corporation United Technologies Research Center Attn: Dr. William M. Foley	1	
Library	1	
400 Main Street East Hartford, CT 06108		
Vought Systems Division LTV Corporation Attn: MDS-T-Library	1	
P.O. Box 5907 Dallas, TX 75222		

NDW-NSWC(W)-5605/1 (Rev. 1-75)

TO AID IN UPDATING THE DISTRIBUTION LIST FOR NAVAL SURFACE WEAPONS CENTER, WHITE OAK LABORATORY TECHNICAL REPORTS PLEASE COMPLETE THE FORM BELOW:

TO ALL HOLDERS OF NSWC/WOL TR 77-7
by Robert L. P. Voisinet, Code CA-41
DO NOT RETURN THIS FORM IF ALL INFORMATION IS CURRENT

A. FACILITY NAME AND ADDRESS *(OLD) (Show Zip Code)*

NEW ADDRESS *(Show Zip Code)*

B. ATTENTION LINE ADDRESSES:

C.

☐ REMOVE THIS FACILITY FROM THE DISTRIBUTION LIST FOR TECHNICAL REPORTS ON THIS SUBJECT.

D.
NUMBER OF COPIES DESIRED _____

GPO 885-970

DEPARTMENT OF THE NAVY
NAVAL SURFACE WEAPONS CENTER
WHITE OAK, SILVER SPRING, MD. 20910

OFFICIAL BUSINESS
PENALTY FOR PRIVATE USE, $300

POSTAGE AND FEES PAID
DEPARTMENT OF THE NAVY
DOD 316

U.S.MAIL

COMMANDER
NAVAL SURFACE WEAPONS CENTER
WHITE OAK, SILVER SPRING, MARYLAND 20910

ATTENTION: CODE CA-41


78